Foliage Echoes and Sensing in Natural Environments

Chen Ming

Dissertation submitted to the Faculty of the

Virginia Polytechnic Institute and State University

in partial fulfillment of the requirements for the degree of

Doctor of Philosophy

in

Mechanical Engineering

Rolf Müller, Chair

Hongxiao Zhu

John E. Taylor

Andrew J. Kurdila

Alexander Leonessa

August 8, 2017

Blacksburg, Virginia

Keywords: bat biosonar, foliage echoes, computational model

Foliage Echoes and Sensing in Natural Environments

Chen Ming

ABSTRACT (ACADEMIC)

Foliage is very common feature in the habitats of echolocation bats and thus its echoes constitute the major input of bats' sensory systems. Acquiring useful information from vegetation echoes facilitates the bats significantly in the navigation and foraging behaviors. To better understand the foliage echoes, in this dissertation, a computer model was constructed to simulate foliage echoes with following simplifications: approximating leaves as circular disks, leaving out shading effects between leaves, and distributing leaves uniformly in the space. Then one tree can be described with three parameters in the model, leaf radius, orientation, and leaf density, where the first two determine the beampattern of each leaf. Compared with echoes collected from real trees, the simulation echoes are qualitatively accurate, i.e., they match in waveforms and also first-order statistics. Since the ground truth is known in the model, the three parameters were estimated with lasso model by selecting 40 features from each echo. The results have shown that estimation of one parameter with the other two known is usually successful with coefficient of determination close to one, and the classification still has reasonable accuracy when the number of known parameter is reduced to one. Besides, the three simplifications were examined with both experimental and simulation approaches. To assess the acoustic impact of leaf geometry on individual leaves, experiments were carried out by ensonifying leaves from both a single and different species. How the leaves' impulse responses change according to their equivalent radii was investigated. The simulation model

of disks fits the experiments done with real leaves within one species and across species reasonably well. Shading effect is found to exist locally when two disks were 25 cm apart and were both in pulse direction. In addition, the inhomogeneous distribution of leaves was introduced by using the branching patterns of L-system. The evaluation of inhomogeneity in echoes produced with two distributions shows that there is always inhomogeneity in echoes, and L-system model does bring more inhomogeneity but not to the same extent as changes in the relative orientation between sonar beam and foliage do.

GRANT INFORMATION

This work received support from the Biobuild Program at Virginia Tech, the National Science Foundation (NSF), and Naval Engineering Education Center (NEEC).

Foliage Echoes and Sensing in Natural Environments

Chen Ming

ABSTRACT (PUBLIC)

Echolocating bats use ultrasonic waves to navigate and forage at night in the forest. They constantly emit pulses and analyze the returning echoes to perceive the surroundings. Foliage echoes are common and important input of their sensory systems, yet what accessible information is contained in foliage echoes for bats is not fully understood. Hence, this dissertation has built an efficient computer model to compute vegetation echoes. To simplify the problem, leaves with various shapes were approximated as circular disks. Besides, every leaf was assumed to be "visible" to sonar, in other words, even if one leaf was shaded by another in the pulse direction, it can still interact with sonar as if the front leaf didn't exist. Then the leaves were uniformly distributed in the space. With the simplifications above, foliage can be described with three parameters, mean leaf radius, orientation, and leaf density. By varying the three parameters to match features of different trees, a large amount of echoes can be calculated efficiently. Compared with measured echoes from real trees, the simulation echoes are similar with them in terms of waveforms and probability density functions. If producing echoes with two parameters fixed and the third randomly chosen from certain range, the random parameter can be estimated with a linear model, lasso regression model, by extracting features from the echoes as inputs. The estimation is accurate. But if varying one of the two known parameters, the accuracy of estimation is largely reduced. Besides, the three simplifications were examined if they have impact on the simulation results. Impulse responses

from leaf specimens were measured with a bio-mimetic sonar head in the anechoic chamber where noise and unwanted reverberations are largely weakened. Experiments were also carried out for two disks of same size by aligning them in the direction of sound emission to quantify shading effect, which shows that shading effect exists locally. Then branching patterns were introduced to the simulation model using L-system that consists of a set of rules to determine how branches grow. The results demonstrates that the simplifications do affect the model accuracy but the influence may be compensated.

Acknowledgments

I would like to thank my adviser, Dr. Rolf Müller for guiding me over the years. You have set an example of excellence as a researcher, mentor, instructor, and role model.

I would like to thank my committee members for all of their guidance; your ideas, discussion, and feedback have been absolutely invaluable.

I would like to thank my family for their love, encouragement, and support, which has helped me get through difficulties and given me the courage to be everything I want.

I'd like to thank my fellow graduate students and undergraduates both at Virginia Tech and Shandong University. I am very grateful to your contribution to this research and kind encouragement.

I'd like to thank my mother-like instructor and math teacher in middle school, Xiaoping Zhu, who was also my best friend. Meeting you was the turning point of my life. The probability to be distributed into your class was $\frac{1}{6}$, and sometimes I just got all the luck.

I want to thank all the professors I met either in Shandong University or at ASA conferences, especially Dr. Sharon Swartz. Your kind encouragement has always been the power for me.

Finally, I would like to thank the staff at Virginia Tech for making me feel at home. Special thanks to Rhoda, Vicki Taylor, Cathy Hill, Lora Howard, and Gail Coe.

Contents

List of Figures

List of Tables

Chapter 1

Introduction

1.1 Bioinspiration and Bat Biosonar

Biological systems have long been regarded as a valuable source of inspiration and insight for science and engineering. After millions of years' stringent selection processes, the materials and function of bio-systems in nature have been fully proven [1]. Material science benefits from learning creatures in nature. A well-known example is lotus leaves. The super-hydrophobic surfaces have been proved to enable the self-cleaning capabilities of lotus leaves [2], which have opened the possibilities of fabricating superhydrophobic surfaces for a variety of products, such as non-wettable rain wear, paints for kitchen roofs, and windows in high-rise buildings [3]. Successful biosystems in nature also provide many inspirations to researchers, such as our brains. Computer science, the science of building artificial computational systems, has long looked to human brains

for inspiration [4]. Artificial intelligence (AI) researchers are addressing a wide range of problems that include using models inspired by the computation of the brain and explaining them in terms of higher level psychological constructs such as plans and goals [5]. Not only human brains but also the sensory systems in the brains of echolocation bats have been the targets that researchers try to understand and mimic. More than 800 species of echolocating bats continuously use ultrasonic waves to sense their surroundings [6]. Their calls consist of two major types, frequency modulated (FM) sweeps and constant frequency (CF) tones. The dominant frequency of the calls are between 11 kHz [7] to 212 kHz [8]. The minimal detection thresholds can be 0.12 mm for little brown bat (*Myotis lucifugus*) [9], 0.08 and 0.05 mm for the horseshoe bats (*Rhinolophus ferrumequinum* and *Rhinolophus euryale*), and 0.065 mm for *Asellia tridens* [10], respectively. This high resolution in sonar systems allows those bats to detect objects as thin as human hairs and thus mosquitoes and other small insects in complete darkness. For example, Little brown bats can eat up to about 1,200 insects in one night [11]. Compared with this extraordinary performance, they are lightweight to fly. The little brown bats weigh about 10 grams and consumes 1.8 – 3.7 grams of insects each day [11]. However, engineered sonar systems require high power supply yet have lower resolution. A 1.7 m long blimp navigated in the environment with plates about 1 m tall, and the error was about 0.5 m [12, 13]. Unmanned drones and autonomous micro air vehicles (MAV) are experiencing fast development in response to the need to deliver parcels from warehouse to the customers in a few minutes and to investigate the environment without much human effort. There are more than one hundred future uses of drones, not to mention they are being used in many areas. In the environment of those potential uses, foliage is a common feature but challenging sonar target

because each leaf acts as a sound-reflecting facet. Foliage echoes are typically superpositions of contributions from many reflecting facets that are hard to decipher. As a result, current autonomous drones may not be able to navigate successfully within foliage based on sonar. Researchers have developed a self-driving drone that can dip, dart, and dive through trees at 48 km/h (30 mph) [14]. The stereo-vision algorithm has allowed the drone to detect objects and build a full map of its surroundings in real-time. But the testing field of the drone had only a few trees sparsely distributed, which made this a task of avoiding large, discrete obstacles rather than navigating within a foliage. Besides, the height where it flew was below the tree crown, so it was actually avoiding the trunks which are relatively easy obstacles. Current autonomous drones always have to sacrifice one from the other between speed and maneuverability. A small quadrotor can do donuts and figure-eights through an obstacle course of strings and PVC pipes as simulated forest [15]. It was controlled by off-board software, which means it needed people around and was unable to execute tasks in a long distance without monitoring. Motion-capture optical sensors and an on-board inertial measurement unit (IMU) helped it estimate the precise position of obstacles. However, it can't do real-time planning; it took an average of 10 minutes to create a route for the obstacle course with flight speed up to 2 mph. Compared with these autonomous drones, echolocating bats are superior in terms of weight, maneuverability, and capability of avoiding trees in dense forest. They react to the environment input in real-time with high speed and are highly maneuverable. Thus the sensory system of echolocation bats may set an example for autonomous drones.

1.2 Foliage Echoes

Foliage echoes are among the most common echoes that all bat species living in densely vegetated habitats encounter in their daily lives. In technical sonar as well as in the study of bat biosonar, vegetation and other non-prey objects are often referred to as sources of clutter echoes in foraging. Bats have to distinguish target echoes from clutter echoes. For example, echolocating big brown bats (*Eptesicus fuscus*) are able to catch prey in the background of foliage [16]. However, in the context of spatial orientation, echoes from background targets are of interest for bats because they enable obstacle avoidance and can be used to characterize landmarks, which bats need for navigation [17]. The big brown bats have been proved to rely on an acoustic landmark to guide spatial orientation [18]. The bats were first trained to fly through the hole with the presence of the landmark to get a food reward; they could still easily recognize the hole if moving the landmark together with the hole, but would crash into the net more often if the landmark was removed. Natterer's bats can learn to distinguish echoes of conifers from those of broad-leaved trees [19]. After the bats had been trained to recognize impulse responses (IRs) with significantly different roughness, i.e., smooth and rough IRs, they were able to classify one unknown IR spontaneously into one of the two categories. They could achieve a performance of about up to 85% correct choices in the discrimination task, which may enable bats to evaluate complex natural targets, such as vegetation types. A few studies [20–23] have carried out statistical analysis on foliage echoes of measured data from several very different species. Rolf Müller et. al have analyzed the statistical features of echoes from yew and weeping fig, which have big oval and needlelike leaves, respectively. They have concluded that several statistical signal features are invariant sufficiently to allow

a classification of the used example plants [20]. By treating the acoustical landmark identification as a biomimetic random process identification problem, Rolf Müller has developed computational theory for classification which could sustain for a reliable target classification performance [21]. Rather than teasing apart contributions from individual leaves, bats are more likely to use statistical invariants in the echoes that are linked to salient foliage features. Researchers have conducted plant classification from bat-like echolocation signals [23] by collecting echoes from five plant species and employing a standard machine learning algorithm, Support Vector Machines (SVM), as classifier. The results have shown that a linear SVM classifier was able to distinguish between any of the five tested plant species with 80-97% of discrimination accuracy and any other species or group of species. The study of the spectral and temporal statistics of the echoes has led to the conclusion that large scale structures could be most informative [22]. Assuming that the spatial distribution of reflectors has the most important influence on the temporal statistics, they have examined the simplest uniform Poisson model to fit the leaf position distribution with point reflectors. As a result, the model worked for certain distance between reflectors for different species. They have also tried a clustered model with centers of clusters following Poisson distribution and clouds of reflectors in each cluster created with Gaussian distribution. It worked especially well for conifers but not very well for broad-leaved trees.

In agriculture, ultrasonic sensors allow an air blast sprayer to spray exclusively where vegetation is detected, and thus study on foliage echoes is an important way to identify vegetation density and plant structures [24–26]. Li et al. [25] have put layered leaves in wooden frame and examined the relationship between the leaf density and the acoustic energy, which may guide the orchard

management but fall short on the the number of features (single feature: acoustic energy) extracted from the echo and that of foliage parameters (leaf density). McKerrow et al. [26] have used multiple echo features and described the effect of the structure of small plants on the echoes. Canopy size and height are major concerns in chemical spraying [27, 28]. An vertical array of 10 ultrasonic sensors carried by a pickup truck has been utilized to realize the measurement and real-time information was reported via software [27]. Instead of using an empirical equation [27], researchers have used artificial neural networks to achieve better prediction for dose adjustment in pesticide spraying [29]. It has been proved that guidance of ultrasound can save 20% of chemicals compared with the system without it [30]. Different modes of the programmable automatic spraying system could further enhance the spraying efficiency [31]. Ultrasonic sensors have been applied to vineyards [28, 32–34], orchard fruits [30, 31, 35], and citrus [36–38], which have relatively short row spacing. Researchers have also applied the ultrasound sensing in olive trees despite larger spacing (up to 12m) between rows of trees with long-range sensors and larger spacing between sensors [39]. These works may provide practical instructions on chemical spraying and the extractions of weed in agriculture, but may not enhance the understanding of bats' behaviors in forest, which could involve plants that are larger than the dimensions of sonar beams and where multiple foliage parameters instead of plant structure have more crucial influence on echoes.

In summary, the prior research of vegetation echoes about bats adopted the echoes measured from real plants, and thus the number of species was limited because significant effort may have to be made for the experiments. Their statistical analysis has proved that the vegetation echoes can be distinguished with certain features and classifiers. But if the approaches apply to the echoes from

trees with more delicate differences, the effectiveness of the classifiers may be posed to question. In addition, point reflector model may not be suitable for broad-leaved trees. Besides, the studies about foliage echoes in agriculture are either limited in the number of statistical features or that of parameters that describe the foliage itself. This work seeks to take a step forward in each of those areas.

1.3 Research Approach

The first part of this research work is to construct an effective and efficient computer model to simulate foliage echoes, which can mimic a large amount of species. A few simplifications and assumptions are made. First, a tree is considered to only contain leaves distributed uniformly in the space, since leaves are the main reflectors in a plant while branches have been proved to play a minor role [26]. Second, it's also assumed that no shading exists between leaves, which means every leaf is "visible" to sonar. Third, leaves are approximated as circular disks. With these simplifications, the leaf model takes leaf size and orientation into account when calculating the beampattern of individual leaves. The spreading loss is taken out from the model to study if the echoes are still time-variant. Since the true values of the three parameters are known when simulating echoes, they are estimated with lasso regression, which can select most important features from the inputs automatically with a tuning parameter.

The second part of this work has been to examine the effect of the three simplifications on the model one at a time. To assess the influence of leaf geometry, i.e., various shapes and uneven surfaces,

on the acoustic scattering of individual leaves, experiments are carried out in anechoic chamber. Leaf specimens from leatherleaf arrowwood (*Viburnum rhytidophyllum*) and other nine species are ensonified in the chamber where their echoes are recorded and later deconvolved to impulse responses. Besides, two disks are aligned in the pulse direction and ensonified with the same sonar system to study shading effect between them. In addition, inhomogeneous leaf distribution that mimics that of trees in nature is introduced by building the tree with branching patterns from L-systems. Two different tree models, pine and ginkgo, are built to mimic the real trees. Echoes from both uniform and L-system models are compared in terms of inhomogeneity measure for the two tree models.

1.4 Chapter Outline

Chapter 1 - introduction

Chapter 2 - a computer model for biosonar echoes from foliage

Chapter 3 - a simplified model of biosonar echoes from foliage and the properties of natural foliages

Chapter 4 - conclusions

Chapter 2

A computer model for biosonar echoes from foliage

2.1 Abstract

Since many bat species thrive in densely vegetated habitats, echoes from foliage are likely to be of prime importance to the animals' sensory ecology, be it as clutter that masks prey echoes or as sources of information about the environment. To better understand the characteristics of foliage echoes, a new model for the process that generates these signals has been developed. This model takes leaf size and orientation into account by representing the leaves as circular disks of varying diameter. The two added leaf parameters are of potential importance to the sensory ecology of bats, e.g., with respect to landmark recognition and flight guidance along vegetation contours. The

full model is specified by a total of three parameters: leaf density, average leaf size, and average leaf orientation. It assumes that all leaf parameters are independently and identically distributed. Leaf positions were drawn from a uniform probability density function, sizes and orientations each from a Gaussian probability function. The model was found to reproduce the first-order amplitude statistics of measured example echoes and showed time-variant echo properties that depended on foliage parameters. Parameter estimation experiments using lasso regression have demonstrated that a single foliage parameter can be estimated with high accuracy if the other two parameters are known a priori. If only one parameter is known a priori, the other two can still be estimated, but with a reduced accuracy. Lasso regression did not support simultaneous estimation of all three parameters. Nevertheless, these results demonstrate that foliage echoes contain accessible information on foliage type and orientation that could play a role in supporting sensory tasks such as landmark identification and contour following in echolocating bats.

2.2 Introduction

Many bat species perform demanding sensing tasks, such as the detection, localization, and classification of prey and obstacles in dense vegetation based on information provided by highly developed biosonar systems [6, 40]. Compared with bat biosonar, engineered sonar systems used on unmanned aerial vehicles are heavier and bulkier yet they cannot deal with complex targets such as vegetation in forest. For example, navigation based on sonar and other sensors has enabled a blimp to avoid large obstacles, e.g., vertical plates about one meter tall [12], with errors as large as 0.5

m [13]. In contrast to this, bats have been shown to discriminate target range difference between 1 and 3 cm [41].

Vegetation is a prominent feature in the habitat of many echolocating bat species. When capturing prey, echoes from a highly structured background can pose a problem because they can obscure prey echoes and hence reduce hunting success [42]. However, certain vegetation echoes have been shown to provide cues for the identification of flowers with nectar [43] and for the position of fruit in the final localization stage [44].

Similarly, echoes returned from a distributed cloud of scatterers may make it difficult to locate the nearest obstacle or find a passageway through the scatterers. However, foliage echoes could also provide valuable information for navigation by supporting the identification of landmarks [20, 40, 45, 46]. It has been shown that Natterer's bats learn to distinguish conifers from broad-leaved trees [19].

Although vegetation echoes are obviously important to the function of bat biosonar, previous studies have either been limited to a small sample of measured data [20–23] or have used a model based on point scatterers [22] that cannot capture the influence of leaf size and orientation on the echoes. In current work, we propose a computational model for foliage echoes that can account for the distribution, size, and orientation of the leaves. Since it has been shown that branches typically contribute little to foliage echoes [26], the ability of the proposed model to capture an extended set of leaf properties should give research into the opportunities and challenges for biosonar that are posed by foliage echoes. The goal of this work is to provide a new powerful tool for creating large ensembles of realistic echoes to mimic different biosonar sensing scenarios that are involved

in foliage echoes.

To achieve this goal in a parsimonious fashion, our model uses only three parameters related to the expected values of leaf density, size, and orientation. We demonstrate the utility of this approach by estimating all of these parameters from the model echoes. This allows an assessment of whether all three parameters influence the echo waveforms and could hence potentially impact the operation of bat biosonar systems in foliage - be it as information-bearing or nuisance signals.

2.3 Materials and methods

2.3.1 Model

To arrive at a parsimonious model for the generation of foliage echoes, the following simplifying assumptions have been made in the work reported here:

First, the foliages consisted solely of isolated reflecting facets ("leaves"), i.e., the model did not include any other plant parts such as branches or trunks. Second, multi-path transmission and shading between leaves was ignored. Third, all individual leaf shapes were approximated by acoustically hard, flat, circular discs that are completely characterized by their radius, position, and orientation in space. Fourth, leaves were distributed uniformly in the foliage whereas their distribution in real foliages could be inhomogeneous, e.g., due to branching patterns. Here, all leaves are distributed uniformly inside a rectangular box positioned one meter away from the sonar along the direction of the sonar's aim. The values of the other two parameters were independently identically distributed

Gaussian random variables. To further simplify the model, it was assumed that the standard deviation for the Gaussian distribution of the leaf radii was tied to the mean. It was taken to be one tenth of the mean. In this way, leaves that were larger on average also varied more in size. The standard deviation of the orientation angle of the leaf was fixed at a value of 5°. Under these assumptions, the simplified model foliages can be described by three parameters: the mean leaf radius r, leaf density ρ (number of leaves per cubic meter) and mean leaf orientation α (Fig 2.1). The angle to describe leaf orientation was chosen as the angle between the surface normal of the leaf and the pointing direction of the sonar.

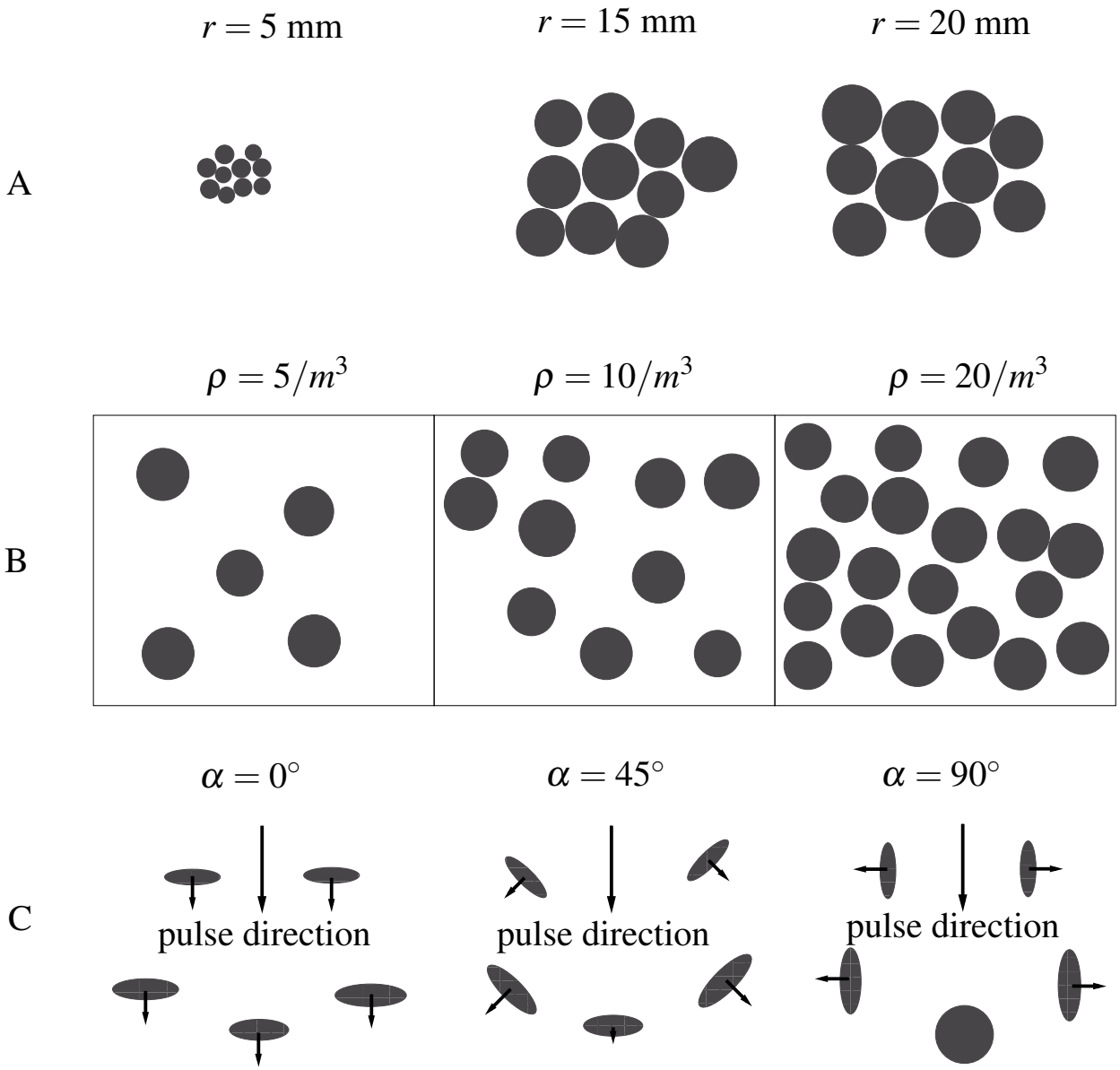

Figure 2.1: Parameters of the proposed foliage model. A) Expected value of the leaf radius r. The radii of all leaves are drawn independently from Gaussian distribution with mean r and standard deviation $\frac{r}{10}$. Ten leaves are shown each for mean radii that equal 5, 15, and 20 mm, respectively. B) Leaf density ρ. Orthogonal projections on the xy-plane of a cubic volume (1 m^3) filled with 5, 10, and 20 leaves are shown, respectively. The frame represents the borders of the cubic volume. C) Orientations in a leaf sample around mean orientation angles (α) of 0, 45, and 90°, respectively. The orientation angle is defined as the angle between leaf normal and the direction the sonar is aimed in, orientations are drawn from Gaussian distribution with mean α and a fixed standard deviation of $5°$.

For plane waves incident on an acoustically hard circular disc at an angle ζ with the surface normal, the scattered field, V^s, is given in the far field as

$$V^s \sim \frac{e^{ikd}}{kd} S, \tag{2.1}$$

where d is the distance between sonar and disc, k is the wave number, and S is the far field coefficient. The far field coefficient S can be expressed as an infinite sum of spheroidal wave functions as follows [47]:

$$S = 2i \sum_{m=0}^{\infty} \sum_{n=m}^{\infty} \frac{\epsilon_m}{\widetilde{N}_{mn}} \frac{R_{mn}^{(1)'}(-ikr, i0)}{R_{mn}^{(3)'}(-ikr, i0)} S_{mn}(-ikr, \cos\zeta) S_{mn}(-ikr, \eta) \cos m\phi, \tag{2.2}$$

where r is the radius of the disc, $k = \frac{2\pi}{\lambda}$ the wave number, $S_{mn}(-ikr, \eta)$ are oblate spheroidal angle functions of the first kind, of order m, and degree n, $R_{mn}^{(1)'}(-ikr, i0)$ is the derivative of the oblate radial functions of the first kind, of order m, and degree n, $R_{mn}^{(3)'}(-ikr, i0)$ is the derivative of the oblate radial functions of the third kind, order m, and degree n, ϵ_m is the Neumann symbol, (η, ξ, ϕ) is the position of observation point in oblate spheroidal coordinates, and $\widetilde{N}_{mn}$ is a normalization constant.

To evaluate the scattered field of discs with different radii over the frequency range of interest here (60 to 80 kHz, modeled after the second/strongest harmonic in the biosonar pulses of the greater horseshoe bat, *Rhinolophus ferrumequinum* [48]), the following procedure was used: For each value of kr, the numerical values of the far-field coefficient S (Eq. 2.2) were calculated for 1000 evenly spaced values of incident angle between 0° to 90° (Fig 2.2A) by numerical evaluation of a

truncated version of the series in Eq. 2.2 [49]. The series coefficients decay exponentially and were truncated based on a magnitude threshold [49]. Since calculating the scattered field of a single disc in this way takes several days on a standard work station, a more time-efficient approximation of the numerical solution with cosine functions was used to obtain all the scattered field values for the different disc diameters and incident angles. The cosine function used for this approximation was of the form $a\cos(b\theta)$, where the amplitude a and the angular frequency b were used as fitting parameters. A nonlinear least squares method based on a trust-region-reflective algorithm [50] was used to accomplish this fit. These fits resulted in data sets containing values for the parameters a and b for each value of the product kr (Fig 2.2B and C). In order to be able to arrive at values for the parameter a and b for any value of kr without much computational cost, power functions were fitted to the relationships between the parameters and kr. This fit was carried out using the same method as described above. The fitting functions used were $a(kr) = \frac{1}{2}(kr)^2 + 0.7$ (i.e., a second order polynomial), and $b(kr) = 0.4(kr)^{-0.9} + 1$, respectively (Fig 2.2B and C).

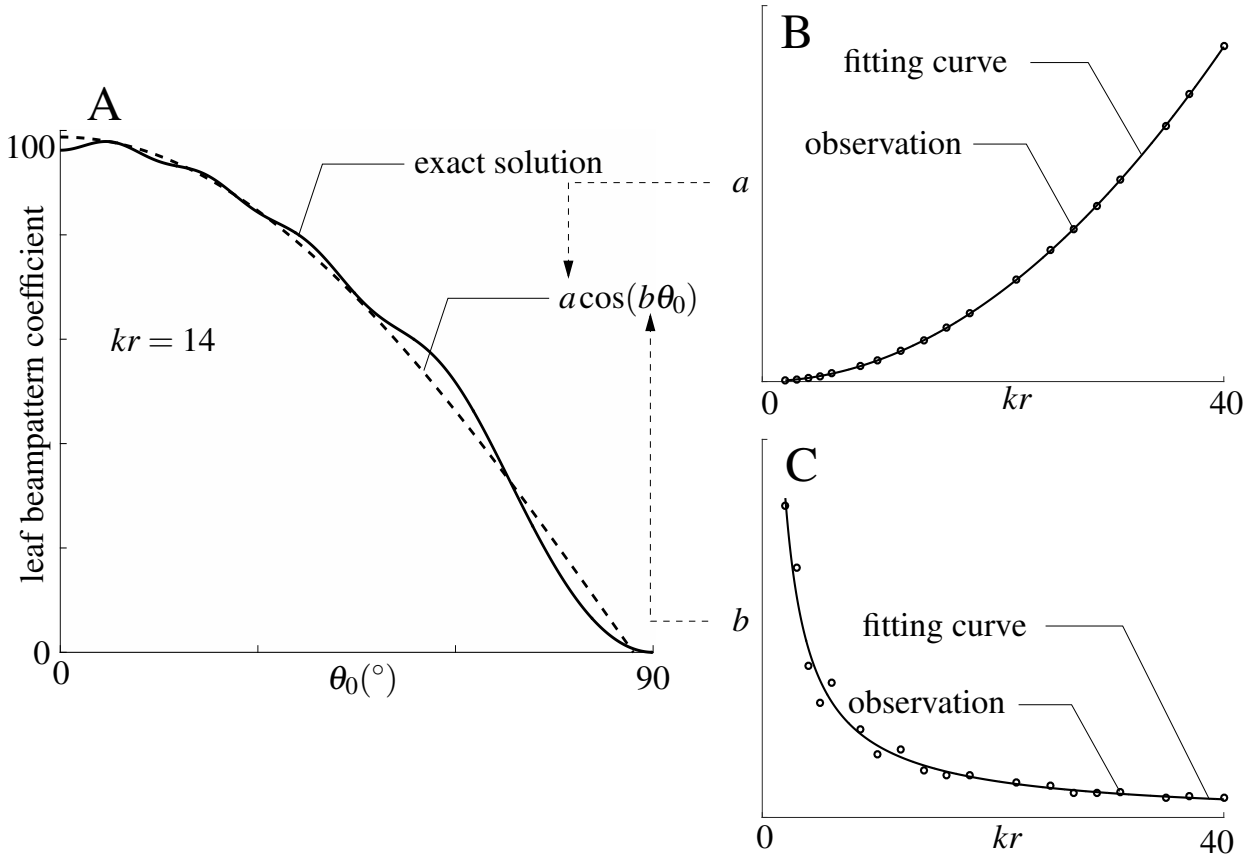

Figure 2.2: Approximation to the scattering beampattern of a disc. A) evaluation of the truncated infinite series for the leaf beampattern coefficient (Eq. 2.2) and its approximation using a cosine function; solid line: series evaluation ; dashed line: cosine fit ($a\cos(b\theta_0)$). The result from the infinite series and the cosine approximation are shown as a function of incident angle θ_0 (0° to 90°) for the case of $kr = 14$, where k is wave number and r is the leaf radius. B) and C) Fitting curves used to determine the amplitude a and angular frequency b of the cosine fit as a function of kr. Open circles: parameter values determined from evaluating a truncated version of the infinite series; solid lines: curve fitted to the data points marked with the open circles.

The shape of the bat biosonar beampattern was approximated by the product of two Gaussians, one a function of azimuth and the another a function of elevation. The sonar was assumed to be monostatic, i.e., emitter and receiver were in the exactly same position which can be justified since the small sizes of bat heads (a few centimeters diameter at most) will not result in a substantial parallax when looking at targets at a distance of one meter or more. The standard deviations of the

Gaussian functions used to model the beampattern in azimuth and in elevation were fixed at the same value of 17.2° corresponding to a -3 dB beamwidth of approximately 30°. The beampatterns' direction of maximum gain was aligned with the normal to one of the surfaces of the rectangular domain in which the leaves were distributed (Fig 2.3).

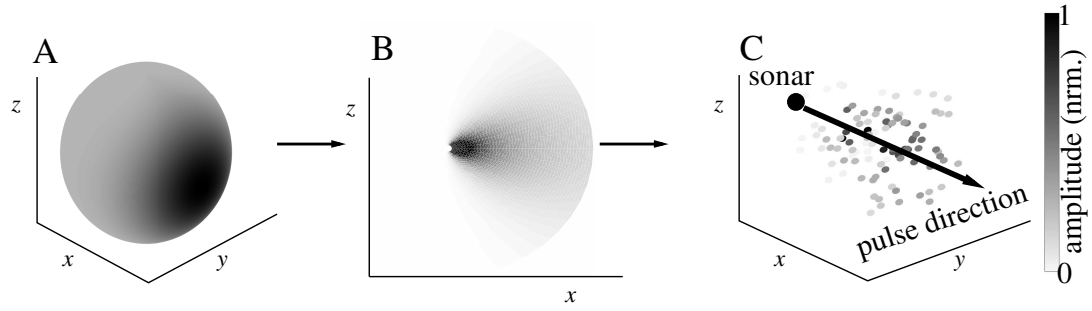

Figure 2.3: Biosonar beampattern model: A) distribution of beam gain amplitude over direction (-3 dB beamwidth 30°); B) distribution of sonar gains in the xz-plane showing directionality gains and spreading losses; C) total (emission and reception) sonar gain mapped on a cluster of leaves representing leaves in a foliage. The axis of maximum beamgain of the sonar is aligned with the $+x$ direction. Leaves are uniformly distributed. Beamgain amplitudes are normalized and encoded by gray scale.

The boundaries of the cuboid-shaped spatial domain over which discs (leaves) were randomly placed to be included in the calculation of the echoes were determined based on the expected maximum gain for the respective position. Positions for which losses due to beamgain and spreading amounted to a drop of more than -80 dB in amplitude were not included (Fig 2.4). This reasoning was based on the dynamic range of the sonar in greater horseshoe bats for which an emission level of around 100 dB SPL in a distance of 10 cm [51] and a hearing threshold around 10 dB SPL [52] have been reported and the assumption that the target strength of the leaves typically does not exceed -10 dB substantially (the target strength of a disk with 4 cm diameter at a frequency of 75

kHz).

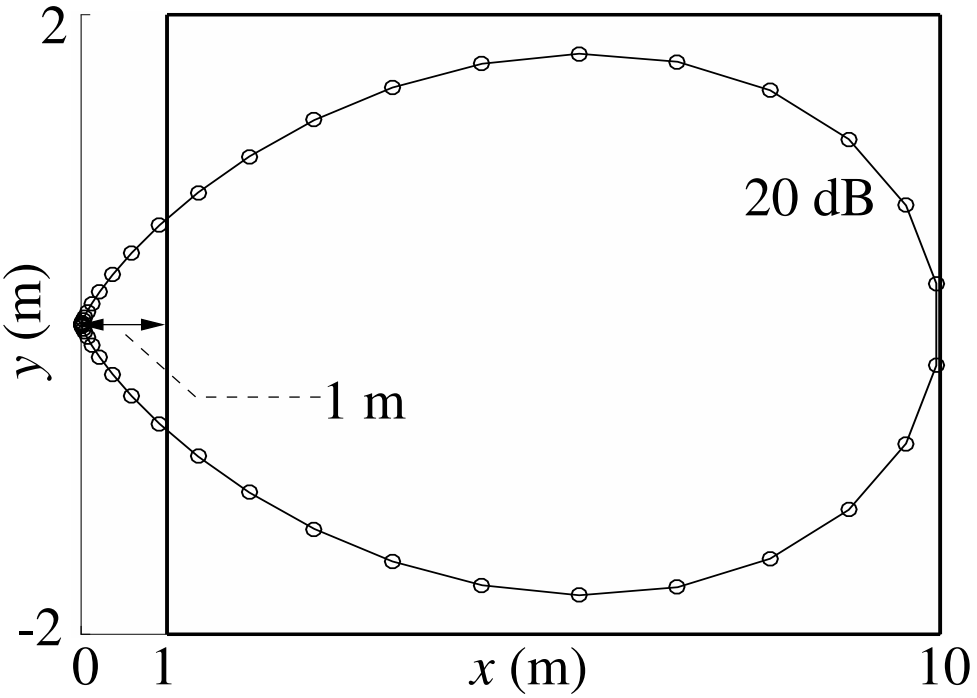

Figure 2.4: Determination of the foliage domain covered by the computations. Iso-gain contour of a sonar beam cross-section for a sound pressure level of 20 dB SPL assuming a source level of 100 dB SPL at 10 cm distance. Emission and reception losses were both considered in these calculations. The Boundaries of the foliage domain cuboid in the xy-plane (solid-line rectangle) were positioned to contain the entire 20 dB SPL iso-gain surface and were rounded up to the next integer multiple of 2 m. The distance between sonar and the cuboid was set to 1 m to ensure the far-field assumption made in the calculation of the scattering from leaves was valid.

The distance between sonar and leaf domain was set to 1 m in order to ensure that the far-field assumption in the calculation of leaf beampattern is valid. The far-field distance for emissions from greater horseshoe bats with call frequency 83 kHz and noseleaf width 8.1 mm [53] would be 3.2 cm. For the ears, an ear length of about 2.2 cm would results in a transition to the far-field at approximately 24 cm [54].

The sonar pulse was assumed to have a power spectrum that was flat between 60-80 kHz. To

acquire the output signal which was an impulse response of ensonified leaves in the model, the frequency domain signal of each leaf in 60-80 kHz range was first calculated with the sonar beampattern and the approximated leaf beampattern according to the leaf's position and orientation relative to the sonar. Responses at other frequencies were set to zero. Then the frequency responses of all leaves were superpositioned. Finally, the inverse Fourier transform was applied to obtain the time domain signal.

2.3.2 Estimation of foliage parameters

Lasso regression was used to estimate the values of the foliage parameters from the resulting echoes. The parameter estimates were linear combinations of the weighted echo features. Finding the weights for the best-trained model was accomplished using two objectives: The first objective was to minimize the sum of the parameter estimate errors in square sense over the observations and the second objective was to keep the sum of the absolute values of the weights at less than or equal to a tuning parameter. The best value for the tuning parameter was determined by virtue of a cross validation approach [55].

A total of 40 features were extracted from each echo for the purpose of estimating the underlying parameters of the foliage model (Fig 2.5). One group of these parameters contained measures of the distribution of the envelope magnitude values taken over the entire echo. Similarly, measures of how the peaks in the echo amplitude were distributed in time over the entire echo were used as a basis for estimating the foliage model parameters. The remaining features were measures derived

from the distribution of envelope magnitudes within ten time windows of even length that spanned the entire duration of the echo.

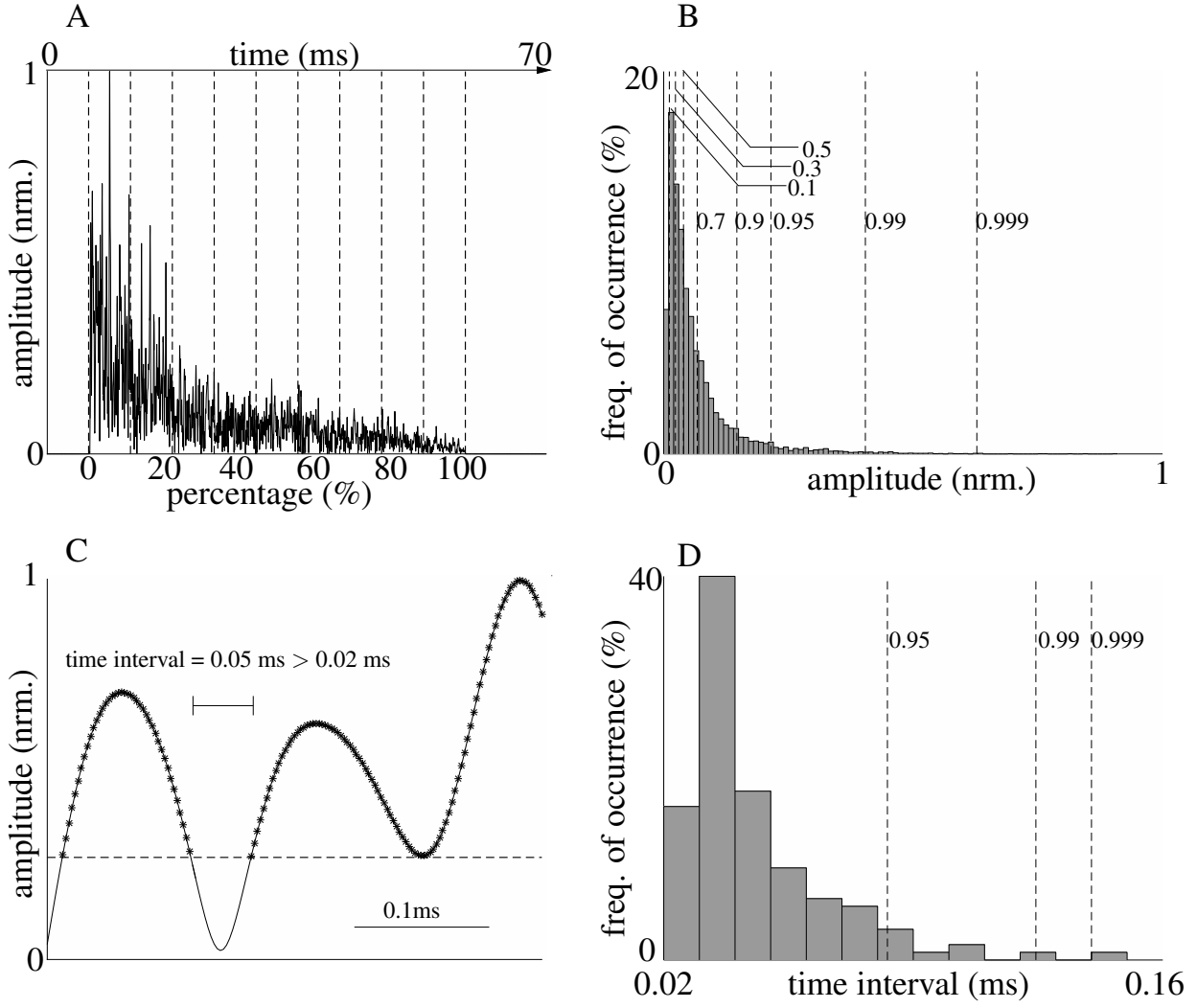

Figure 2.5: Part of the echoes' statistical features. A) The envelope of an echo which was evenly divided into 10 parts. B) [0.1, 0.3, 0.5, 0.7, 0.9, 0.95, 0.99, 0.999] quantiles of the amplitude above threshold, which is one tenth of the maximum value in the last window (90% to 100%). C) An example of time interval longer than 0.02 ms in zoomed-in view of the envelope. The time intervals are time difference of two adjacent points whose values are larger than the threshold mentioned above. Find all time intervals and keep the ones longer than 0.02 ms. D) [0.95, 0.99, 0.999] quantiles of the time intervals longer than 0.02 ms.

For features derived from the echo envelope amplitudes, a threshold of one tenth of the maximum

envelope magnitude in the last time window was set to exclude features associated with very small magnitude values from these calculations. The following features were derived from the magnitudes of the envelope of the entire signal: area under the envelope, quantiles (0.1, 0.3, 0.5, 0.7, 0.9, 0.95, 0.99, 0.999) of magnitude values that were larger than the magnitude threshold, central moments (2nd to 5th) of the above-threshold magnitude values, the same four central moments for time intervals longer than a 20 μs threshold. The time-differences were measured between neighboring points in the signal envelope that were higher than the threshold, and a set of quantiles (0.95, 0.99, 0.999) of those selected time intervals. The quantiles were used to describe the shape of the probability density function (pdf) of those magnitudes. The 2nd central moment is the variance and the scaled version of third central moment is skewness, a measure of the lopsidedness of the distribution. The scaled version of fourth central moment is kurtosis and serves as a measure of the heaviness of the tail of the distribution. Features calculated within the 10 time windows were: the number of magnitude values larger than the threshold in each window and mean value of the magnitudes above the threshold in each window.

Cross validation was used to find the tuning parameter and avoid overfitting. It was carried out using 80% of the echoes. This cross-validation echo data set was divided into 10 subsets of equal size. One subset was excluded and the lasso model was fitted to the remaining nine subsets of the echoes. Then the model was tested on the excluded subset. The process was repeated 10 times in total where each time a different subset was excluded. The estimation errors made over all these 10 tests were summed and used to determine the value of tuning parameter that resulted in the minimum error.

With this cross validation followed by the lasso regression itself, foliage parameter estimates were carried out for the following three scenarios: (i) estimation of a single unknown foliage parameter with the other two parameters fixed, (ii) estimation of one foliage parameter with the second parameter fixed and the third parameter left to assume unknown and variable values, and (iii) estimation of one parameter with the other two parameters remaining unknown and subject to change.

In all these estimation scenarios, the following values were used for the known/fixed parameters: leaf density 100/m^3, mean orientation angle 7°, and mean leaf radius 15 mm. Parameters left unknown were drawn randomly from the values in the following sets in each echo: leaf density [20, 100, 200, 300, 500]/m^3, mean orientation angle [0, 20, 40, 60, 80]°, and mean leaf radius [7, 10, 13, 17] mm. Parameters to be estimated were left to take any integer within the following intervals: leaf density [20, 500]m^3, mean orientation angle $[0, 90]^\circ$, and mean leaf radius [5, 20]mm. For the estimation of a single unknown parameter, 100 echoes each were generated for 100 different parameter combinations. As described above, 80 of these echoes were used for training and the remaining ones were used to test the lasso model. For the estimation of parameters in other situations, 500 echoes were generated from 100 parameter combinations with 5 echoes from each. Among those echoes 400 were used in training, and the remaining 100 echoes were used in testing.

2.3.3 Field echo recordings

The impulse responses from real trees were recorded for comparison with the simulated echoes. Recording of the echoes in the field was carried out using a biomimetic sonar head. The sonar

head used a single electrostatic ultrasonic loudspeaker (Series 600 open face ultrasonic sensor, SensComp, Inc., Livonia, MI, USA) with a two-sided -3 dB beamwidth of 10° at 50 kHz. A power amplifier (AA-301HS, A.A. Lab Systems Ltd. Ramat-Gan, Israel) was used to drive the loudspeaker. Two MEMS capacitive microphones (SPU0410LR5H, Knowles Electronics, LLC. Itasca, IL USA) mounted on pre-amplifier boards (Momimic, Dodotronic, Rome, Italy) were used for signal reception. An A/D and D/A conversion board (NI-6351, National Instruments Corp., Austin, TX USA) was used in the setup and provided 16-bit resolution and 500 kHz sampling rate for digital-to-analog and analog-to-digital conversion. The sonar head was mounted on a tripod, the height of which above ground was adjusted according to different trees to let the transmitted signal hit the foliage at an approximately normal incident angle. The emitted signal consisted of a 5-ms-long linearly modulated chirp covering a frequency band from 20 to 100 kHz. The experiments were done on Virginia Tech's campus, and no endangered or protected species were involved. No specific permissions were required.

2.3.4 Comparison of simulation results with field recordings

The echoes of two different tree species were recorded for comparison to the simulated echoes: Japanese maple (*Acer palmatum*) and coniferous tree, arborvitae (*Thuja occidentalis*). Echoes were obtained from one tree per species. 400 echoes (200 per microphone) were collected per viewing angle with a total of 5 viewing angles for each tree. 30 leaf samples [56] were collected from 4 branches at different heights for Japanese maple. The mean leaf area over 30 leaves was obtained by calculating the area of each leaf after scanning it and counting the dark (green) pixels.

The equivalent leaf radius that produced the same area for a circular disk was used to determine the mean leaf radius of the model, which was 1.46 cm. Mean orientation angle and density were decided based on observation. The foliage of Japanese maple consisted of dense leaves with mean orientation angle about $45°$, and thus the density was set to 5000/m^3. The arborvitae had foliage with forms of flat sprays with scale-like leaves; in the model, 1 mm, $45°$, and 10000/m^3 were used to represent its mean leaf radius, orientation angle, and leaf density, respectively. The measured echoes were first filtered with passband 20–110 kHz, then cross-correlated with emitted signal to acquire the impulse response, and filtered again with passband 60–80 kHz to match the frequency range in simulation.

In the simulation that were designed to mimic the measured tree foliages, the length of the foliage domain along the sonar's line of sight was set to match the pulse duration observed in the field recordings. The distance between the sonar head and nearest leaf was determined from the first point in time where the echo amplitudes clearly exceeded the noise amplitudes. The same distance was then used in the respective simulations. The -3 dB sonar beamwidth for these simulations was set to $10°$ to match the beamwidth of the experimental setup.

For a quantitative comparison between the simulated and the measured foliage echoes, each echo was divided into three time windows of equal length. In each of these windows, a histogram estimate for the probability density function (pdf) of the echo amplitudes was obtained. The difference between pdf estimates for simulated and measured echoes was quantified using the Bhattacharyya distance [57]. The values of the Bhattacharyya distance range from zero to infinity. The smaller the distance is, the better two pdfs match each other. In order to provide a reference for judging

these difference, the differences obtained for simulated versus measured pdfs were compared to the differences found within the simulated and measured data sets. The Kolmogorov-Smirnov test [58] was also conducted to examine the similarity between the amplitude distribution of envelopes from simulated and measured echoes in each of the three windows. The envelopes were calculated with Hilbert transform. Since the sampling frequency of the simulation and field recordings were different, the echoes were both downsampled to 100 kHz before the envelopes were calculated.

2.4 Results

2.4.1 Comparison of real echoes and simulation

The waveforms of the measured and simulated echoes were found to be qualitatively very similar to each other for the two tree species/specimens studied (Fig 2.6). This impression was confirmed by quantitative comparisons of the first-order probability density functions obtained for the signal amplitudes. The Bhattacharyya distances used for this purpose were fairly similar for comparisons within the simulated and measured echoes on the one hand and comparisons between these two data groups on the other. For example, in the central time windows of the echoes from the arborvitae, the average Bhattacharyya distance between pdfs of simulated echoes was 0.03 (± 0.02 standard deviation, $N = 5$) that between pdfs of measured echoes was 0.04 (± 0.02 standard deviation, $N = 5$), and that between simulated and measured echoes was 0.03 (± 0.02 standard deviation, $N = 5$, Fig 2.7). The Kolmogorov-Smirnov test for each of the three windows resulted

p-values as 0.55, 0.99, and 0.70, respectively, which indicated that the probability distributions of the envelopes of simulated and measured echoes were the same.

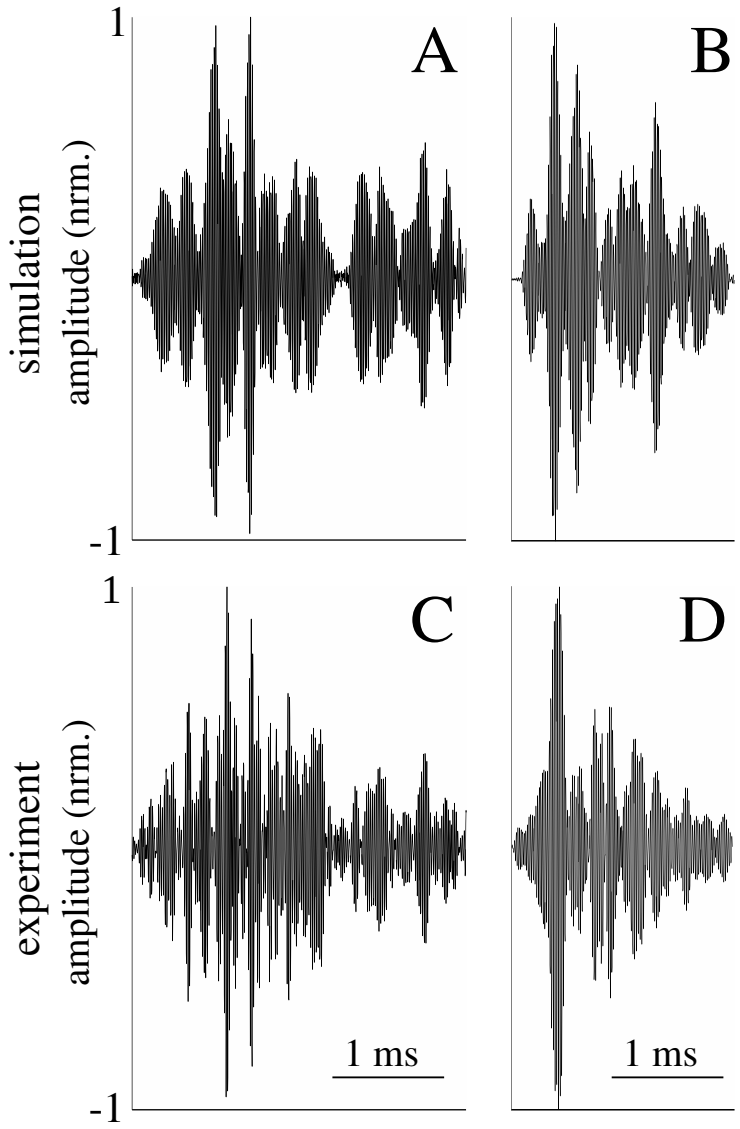

Figure 2.6: Comparison between examples of simulated and measured echoes. A-B) Simulated echoes: A) with parameters similar to the Japanese maple specimen: mean leaf radius 1.46 cm, density 5000/m^3, and mean orientation angle 45°. B) with parameters similar to the arborvitae specimen: mean leaf radius 0.1 cm, density 10000/m^3, and mean orientation angle 45°. C-D) echoes measured in the field: C) Japanese maple, D) arborvitae. All echo amplitudes were normalized to their respective maximum.

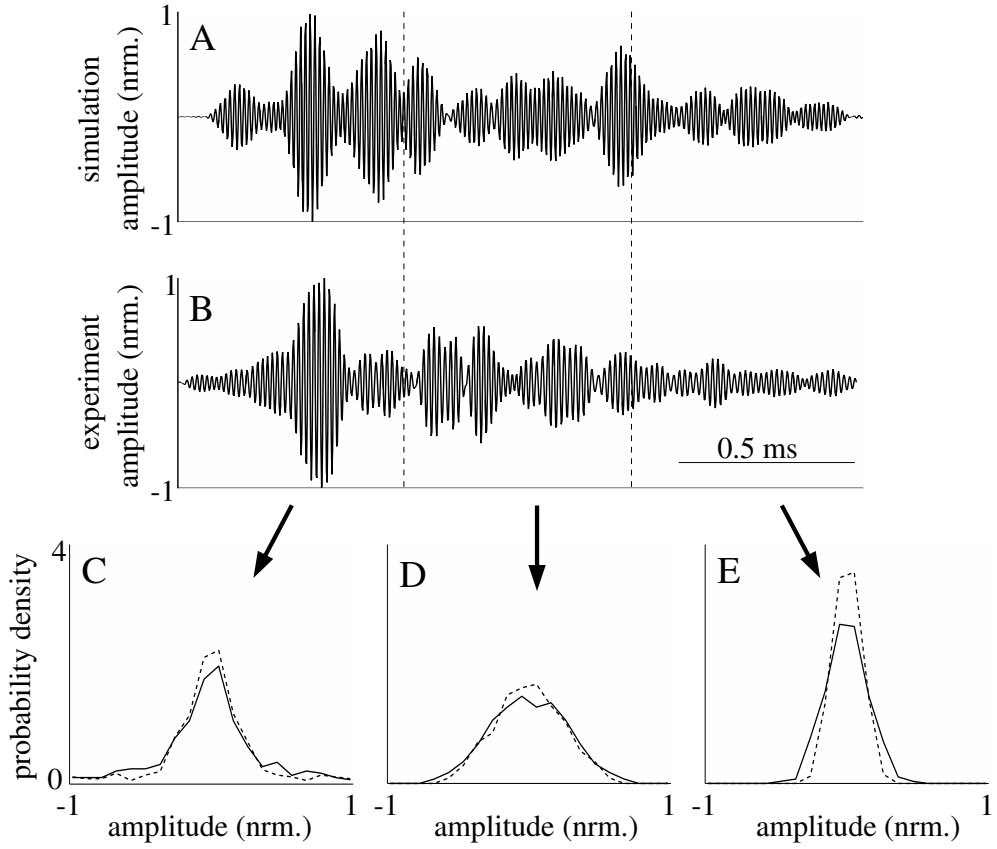

Figure 2.7: Comparison of probability density functions for the amplitudes of simulated and measured echoes: A) simulated echo produced by a model with parameters adjusted to mimic arborvitae. B) echo from the same species measured in the field. The simulated and measured echoes were segmented into three time windows of equal length, the probability density functions for the amplitudes in each segment are shown in C), D), and E). Solid lines: simulated echoes; dashed lines: measured echoes.

2.4.2 Time-varying echo properties

The most visible time-variant property of the echoes (simulated or measured) was a decay in echo amplitude with increasing time due to geometric attenuation. That was reflected by amplitude probability density functions with decreasing spread over time (Fig 2.7). However, after the effects of the geometric spreading losses were removed from the echoes, the resulting amplitudes

remained time-variant but with a reverse dependence where the spread of the amplitude probability functions tended to increase with time (Figs 2.8 and 2.9). This remaining non-stationary behavior of the echoes was quantified using the Bhattacharyya distance as a difference measure for probability density functions associated with different times during the echoes. This analysis provided evidence that the time-variant behavior of the probability density functions was linked to the properties of the model foliages: For example, among all the Bhattacharyya distances obtained between probability density functions obtained for different time windows positioned within the central 80% of the echo durations, the 95%-percentile of the differences increased by 40% (from 0.1 to 0.14) as the leaf density was increased from $20/m^3$ to $500/m^3$. Hence, in this case, the 5% largest differences between the probability density functions increased as the model foliages (mean leaf radius: 5mm, mean leaf orientation: 90°) became denser. Likewise, the Bhattacharyya distances were also found to depend on leaf orientation: As the average leaf orientation was changed from 0° to 90°, the 95%-percentile of the Bhattacharyya distance was reduced by 50% from 0.24 to 0.12. Hence, the time variance was greater when the leaves were oriented with respect to the sonar's light of sight.

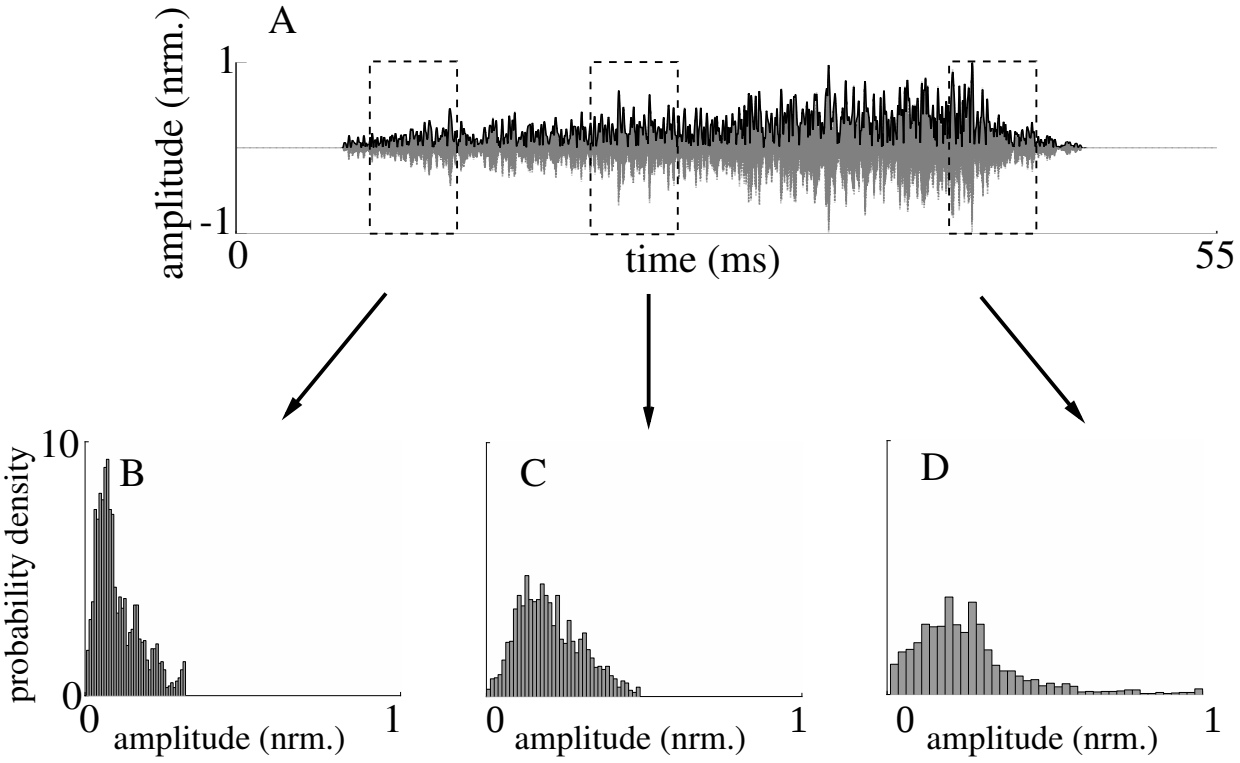

Figure 2.8: Example of time-varying echo and its probability density functions in three different windows. A) simulated echo waveform with envelope (black) computed without inclusion of spreading losses. B), C), and D) probability density function for the three time windows shown in A).

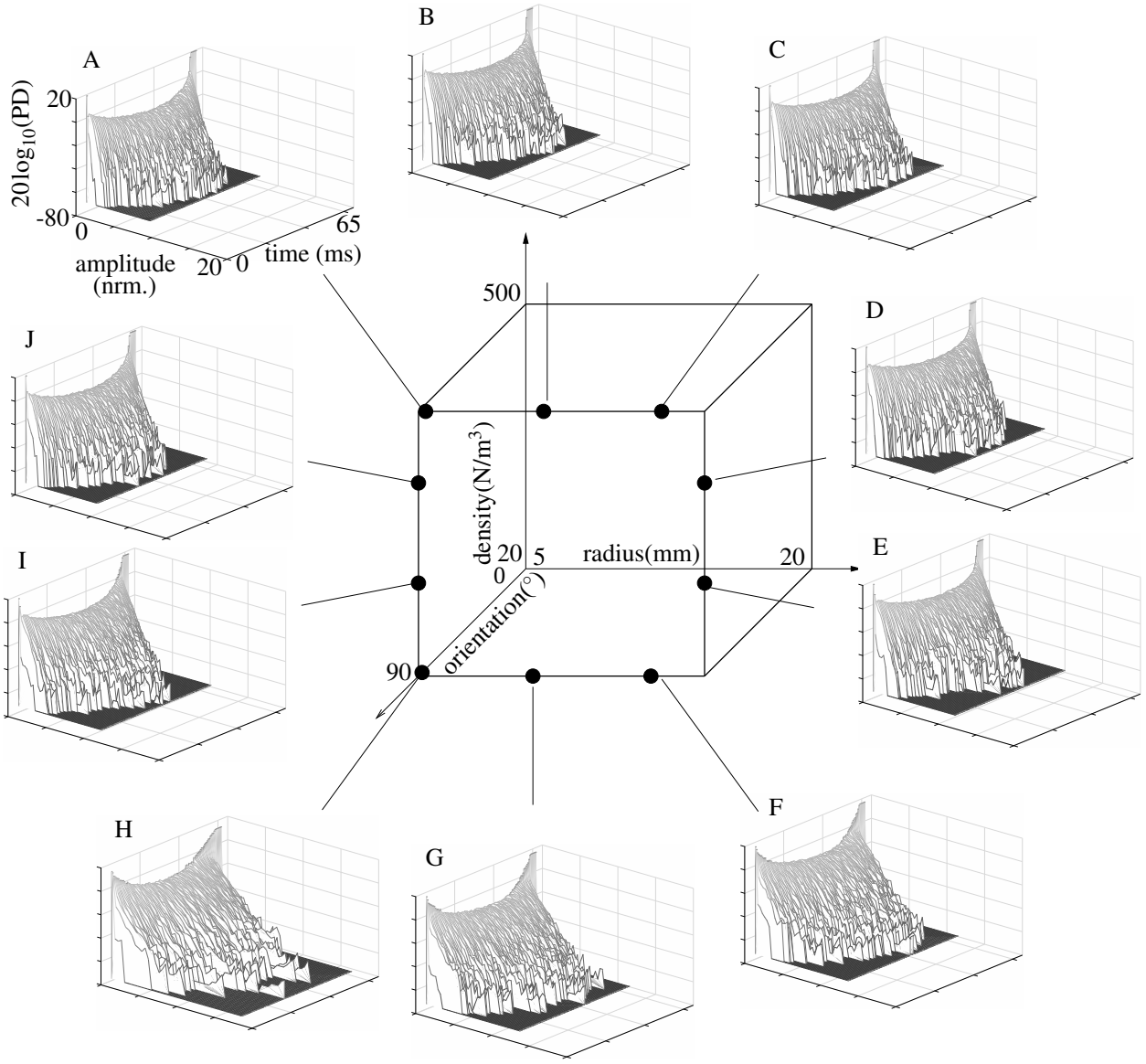

Figure 2.9: Time-varying nature of the foliage echoes: logarithm of the probability density ($20\log_{10}$(PD)) of the echo envelope amplitude as a function of time. The data set used for each plot contains 100 echoes each of which was normalized to the the maximum root-mean-square level within the respective data set. A-J) probability density functions for different points in the foliage models feature space (center).

2.4.3 Parameter estimation

It was found that accurate estimation of a single unknown foliage parameter was readily achievable with the lasso regression method employed (Fig 2.10). For all three parameters of the model, the estimates were highly correlated to the actual values (r^2 values: 0.99, 0.98, and 0.98 for leaf density, mean leaf orientation, and mean leaf radius, respectively). For the estimation of one foliage parameter where one of the other two parameters is known and the other remains unknown, all six possible scenarios yielded correlations between the true parameters and the estimates that were lower than those obtained for single unknown parameters with most r^2 values falling between 0.5 and 0.6 (Fig 2.11). An exception was the estimation of leaf radius with known leaf density and unknown average orientation, where an r^2 value of 0.9 was reached (Fig 2.11E). Finally, estimation of one parameter was attempted with the other two parameters unknown, these estimates were poorly correlated with the actual parameters and hence did not provide much useful information of foliage features.

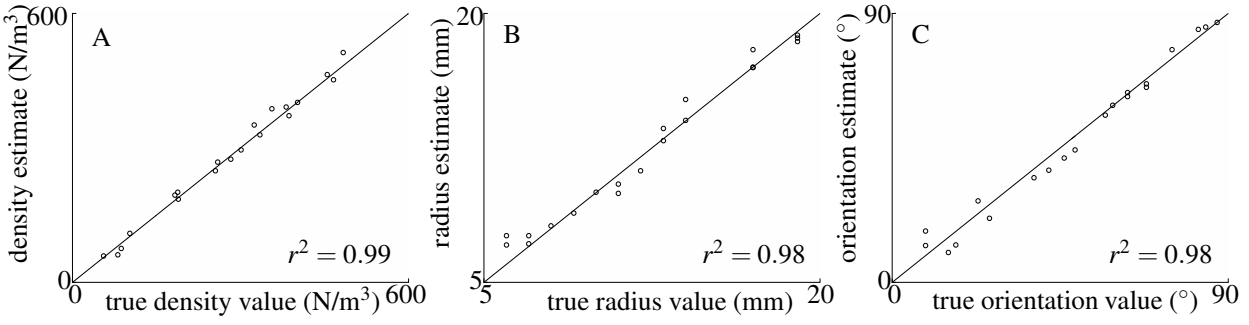

Figure 2.10: Estimation of a single model parameter with the other two parameters fixed and known. Estimates of A) leaf density ρ, B) mean leaf radius r, and C) mean leaf orientation α. Whenever a parameter was assumed to be fixed at a known value, leaf density, mean leaf radius, and mean leaf orientation were set to $100/m^3$, 1.5 cm, and 7°, respectively. The coefficient of determination is indicated in the bottom right corner for each estimation.

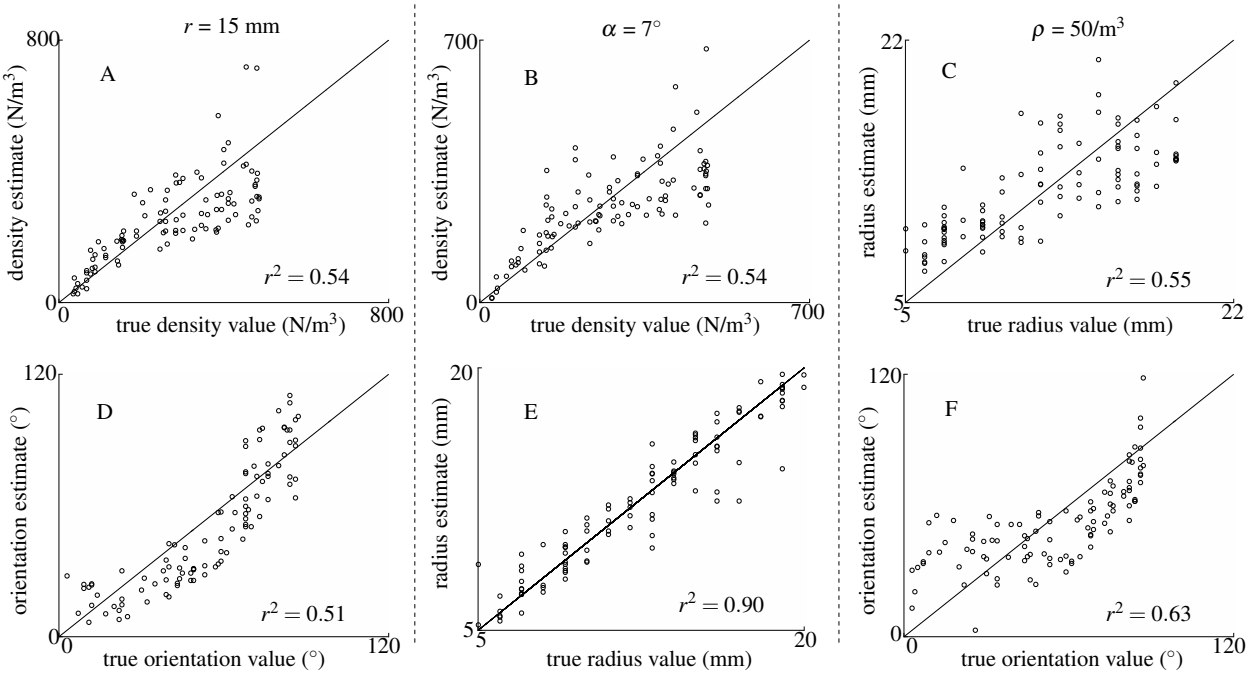

Figure 2.11: Estimates of a single model parameters with one known and one unknown parameter: A) estimates of leaf density ρ with mean leaf radius r fixed, B) estimates of leaf density ρ with average leaf orientation α fixed, C) estimates of leaf radius r with leaf density fixed, D) estimates of average leaf orientation α with leaf radius r fixed, E) estimates of leaf radius r with average leaf orientation α fixed, F) estimates of average leaf orientation α with leaf density ρ fixed. Whenever a parameter was fixed to a known value, $100/m^3$, 1.5 cm, and 7° were used for leaf density, mean leaf radius, and mean leaf orientation, respectively. Whenever a parameter was left unknown and free to change, it was selected randomly from the values in the following sets for each echo: leaf density [20, 100, 200, 300, 500]$/m^3$, mean orientation angle [0, 20, 40, 60, 80]°, and mean leaf radius [7, 10, 13, 17] mm. The coefficient of determination is indicated in the bottom right corner for each estimation.

2.5 Discussion

The novelty of the foliage model presented here lies in the use of discs to approximate the acoustic scattering behavior of the leaves. This introduces two additional parameters, leaf size and leaf orientation, that are not needed in models based on omnidirectional point scatterers [22]. While

addition of these parameters makes the model more complicated, both of these foliage parameters could be of importance to the sensory ecology of bats: Being able to estimate the average size of the leaves in a foliage could help bats to identify the type (e.g., the species) of trees or bushes they encounter. The ability to tell the type of a foliage from the echoes could, in turn, support the recognition of individual trees or bushes that may serve as landmarks for navigation. Similarly, the ability to identify foliage types could help the bats to find their food if certain foliage types are more likely associated with the presence of food [43, 44] than others. Leaf orientation could play an important role in guiding the bats' flight path in close proximity to foliage [17], e.g., when the animals are following the contour of a vegetation edge. Since the leaf normals in a foliage are likely to be oriented towards the surface of the foliage, being able to tell the average direction of the leaf surface normals could be a convenient way to determine the orientation of a foliage contour and control the direction of a flight path that follows the contour without collision.

The results presented here demonstrate that estimation of foliage parameters (leaf density, average leaf size and orientation) from the echo waveforms is possible using echo features that could also be accessible to bats in a similar form. However, with the method used here (lasso regression), highly accurate estimation was only possible for a single unknown parameter. Estimation of two unknown parameters yielded results that could still be useful, but provided a much lower accuracy than was the case for a single parameter. Since there is no reason to believe that present results constitute an upper bound on the achievable performance, it remains possible that bats may be able to perform vastly better than the current pilot results. But even if this is not the case, the level of estimator performance demonstrated here could be very helpful to bats in densely vegetated

habitats. For example, a bat may have sufficient *a priori* knowledge about the leaf density and average leaf size in the foliage of its habitat. A bat armed with such accurate *a priori* information would be able to get precise estimates of average leaf orientation that it could use to follow foliage contours within a known habitat. For landmark identification in an uncertain location, bats may be able to determine the orientation of the foliage surface and hence the average orientation of the leaf normals through other means, e.g., by looking at the foliage surface from different directions. Once the average orientation of the leaves is known, the animals could use this *a priori* information to obtain estimates for leaf density and average leaf size to identify a known landmark tree or bush by its foliage type.

Spreading losses for ultrasonic waves traveling in a three-dimensional medium impose strong time-variant signatures onto echoes that originate from a foliage where the reflectors (leaves) are spaced over a wide range of distances from the sonar. However, these effects do not reveal much about the target other than the range at which a certain component of the target's impulse response has originated. However, the same information is already available from the time of flight in a much more reliable fashion since echo amplitude depends on transmission losses as well as target strength whereas time of flight depends only on target range. Hence, the effects of spreading losses on an echo are probably not a prime information-bearing echo features by themselves. The time-variant effects that were found in the model echoes studied here after spreading losses were removed could be more informative than the spreading losses since they were found to depend on all three foliage parameters. No information is available in the literature at the time of writing as to whether bats would be able to sense different time-variant behaviors within an echo waveform. It has been

shown, however, that bats can distinguish smooth and rough echo waveforms [19]. Detecting time-variant changes in an echo waveform could possibly be handled through mechanisms that are similar to detecting the ups and downs in a rough waveform.

In the current work, echoes were simulated within a 20 kHz frequency band that is similar to the strongest harmonic of greater horseshoe bats. This is much narrower than the 115 kHz bandwidth that has been previously used for the classification of vegetation echoes [22, 23]. The results obtained here hence demonstrate that even bat species with fairly "narrow-band" biosonar signals could already have access to detailed information about complex vegetation environments without the need for the high degree of precision that large pulse bandwidths can convey [22, 59].

The simulation model studied here has been simplified by neglecting properties of natural foliages such as variable leaf geometries, acoustic shading of one leaf by another, multipath sound propagation across multiple leaves, and inhomogeneities in the spatial distribution of the leaves. It remains to be seen to which extent these factors could effect the characteristics of foliage echoes. Previous findings suggest that adding clusters to the spatial leaf distribution improves the goodness of fit between real data and simulation [22], but a full investigation of the role of leaf inhomogeneity still needs to be undertaken. Similarly, it should be investigated if alternatives to the parameter estimation approach used here suffer from the same limitation on the number of parameters that can be estimated simultaneously or if it would be possible to arrive at accurate estimates for all parameters of an unknown foliage. Sequential estimation could be a candidate methods for achieving this, since it has been demonstrated to add to performance in bioinspired classification of foliage echoes [60]. Bats could even control their motions to enhance the encoding of sensory information

on the foliage [61]. If indeed all three foliage parameters considered here could be estimated without prior knowledge, it would give bats many more opportunities to master the demanding sensory task associated with navigation in complex natural environments.

2.6 Acknowledgments

We thank Philip Caspers for the development of the biomimetic sonar system. We also thank Prof. Susan Day for the instruction on tree species recognition.

Chapter 3

A simplified model of biosonar echoes from foliage and the properties of natural foliages

3.1 Abstract

Foliage echoes could play an important role in the sensory ecology of echolocating bats, but many aspects of their sensory information content remain to be explored. A realistic numerical model for these echoes could support the development of hypotheses for the relationship between foliage properties and echo parameters. In prior work by the authors, a simple foliage model based on circular disks distributed uniformly in space has been developed. In the current work, three key simplifications used in this model have been examined: (i) representing leaves as circular disks, (ii) neglecting shading effects between leaves, and (iii) the uniform spatial distribution of the leaves.

The target strengths of individual leaves and shading between them have been examined in physical experiments, whereas the impact of the spatial leaf distribution has been studied by modifying the numerical model to include leaf distributions according to a biomimetic model for natural branching patterns (L-systems). Leaf samples from a single species (leatherleaf arrowwood) were found to match the relationship between size and target strength of the disk model fairly well, albeit with a large variability part of which could be due to unaccounted geometrical features of the leaves. Shading between leaf-sized disks did occur for distances below 50 cm and could hence impact the echoes. Echoes generated with L-system models in two distinct tree species (ginkgo and pine) showed consistently more temporal inhomogeneity in the envelope amplitudes than a reference with uniform distribution. However, these differences were small compared to effects found in response to changes in the relative orientation of simulated sonar beam and foliage. These findings support the utility of the uniform leaf distribution model and suggest that bats could use temporal inhomogeneities in the echoes to make inferences regarding the relative positioning of their sonar and a foliage.

3.2 Introduction

Many echolocating bat species can navigate [20, 40, 46] in dense vegetation and find insect prey or other foods such as nectar [45] and fruit[44] among foliage based on information obtained from ultrasonic biosonar echoes [16]. Hence, the nature of foliage echoes is likely to play a critical role in the function of the biosonar system of bats that occupy such sensori-ecological niches. Foliage

echoes could serve as sources of information for a variety of sensory tasks: For example, the ability to distinguish different foliage types based on their echoes could support habitat selection or the identification of landmarks. The ability to estimate the average orientation of leaves in a foliage could allow bats to obtain information on the orientation of a foliage surface and hence support following a contour along a vegetation edge. Natural foliages are highly complex (bio)sonar targets that consist of many ultrasound-reflecting facets (esp. leaves). As a consequence, foliage echoes are superpositions of many (tens, hundreds, or even thousands) individual reflections. Because it is not possible in practice to know the position and orientation of all facets that contribute to given foliage echoes, such echoes have to be treated as random processes. It has been demonstrated that bats can distinguish signals with different roughness [19] which indicates that the animals have the ability to distinguish between echoes that are realizations of random processes based on differences in certain statistical invariants. On the computational side, a few studies have demonstrated that the classification of foliages based on echoes is possible [20–23]. These classification studies have typically investigated distinct foliages or foliage categories. Hence, they shed little light on the limits for making finer distinctions between foliages or the ability to estimate continuous foliage parameters (e.g., leaf density or leaf size). Simulation studies based on computational foliage models hold promise for gaining insight into these topics because they allow it to vary foliage parameters continuously or in very small steps where many realizations for each step can be created and the ground truth is always known. A condition for this approach to succeed is that the computational foliage models are able to capture all salient foliage properties accurately. Yovel et al. [22] have presented a foliage model that treats leaves as point reflectors, i.e., each leaf has

an omnidirectional beampattern. The model also tested two different leaf distributions (uniform Poisson and leaf clusters placed with a Poisson model). The results showed that cluster-distribution model provided a better fit to measured echo power spectral densities than the uniform-distribution model. In prior work by the authors, a foliage model includes leaf size and leaf orientation as additional parameters [62]. Given that leaves are likely to fall into the Mie scattering region [63] of the bat biosonar pulses, i.e., the leaves are on a similar size scale as the wavelengths used by the bats, these two parameters can be expected to have a strong impact on the echo contributions of individual leaves. The model developed by the authors predicts that the echoes of the entire foliage are also impacted by those parameters and hence could provide an opportunity to estimate average leaf size and orientation from the echoes. For the insights gained through computational foliage models to be valid for actual foliage echoes and hence the sensory ecology of echolocating bats, it is important that the simplifying assumptions of the model are close enough to reality to replicate the key properties of the echo-generating process accurately. Hence, the goal of the work presented here has been to look into two key features of the model, the disk-shaped leaves and their homogeneous distribution in space. To compare the impact of leaf geometry and size on the scattering properties of the leaves, sample leaves from different plant species were ensonified and their impulse responses were recorded experimentally. As part of these experiments, the extent of shading between leaves was also assessed. To assess whether the uniform leaf distribution model needs to be improved in the light the inhomogeneities that can be found in real tree foliages, especially due to branching patterns and the distribution of leaves along the branches, the foliage model was modified so that the leaves were placed using an established model for tree branching

patterns (Lindenmayer or L-systems). Along with this next generation of the foliage model, a measure for echo inhomogeneities has been developed and applied to quantify the impact of foliage inhomogeneity as well as the orientation of the sonar with respect to a foliage.

3.3 Methods

3.3.1 Model

The computational foliage model studied here simplifies the geometry of the leaves in a foliage as circular discs. The exact far-field solution for the beampattern of an acoustically hard disc can be expressed as a sum over an infinite series composed of spheroidal wave functions. A highly accurate numerical evaluation of the exact solution is possible truncating the series based on a threshold criterion [49]. However, since this approach is computationally expensive, a cosine function was used to approximate the amplitude of the scattered field as a function of leaf size, sound wavelength, and incident angle [62]. In the current work, the positions of leaves in the model foliage were determined in two alternative ways: In the first alternative, the leaves were uniformly distributed in a rectangular box in front of sonar as has been reported previously [62]. In the second alternative, the leaf positions were determined based on a biomimetic branching pattern obtained from a Lindenmayer (L)-system [64] combined with ad-hoc rules for how leaves grow around each branch. For the uniform distribution, the initial leaf domain was a rectangular box with walls placed so that they enclosed the entire volume where the spreading losses associated with two-way

transmission between sonar and each leaf did not exceed 80 dB. For a -3 dB beamwidth of sonar to 30°, this approach resulted a leaf domain with dimensions $9\times4\times4$ m, where all edge lengths were rounded up to the nearest integer. The leaf domain was positioned one meter away from sonar to conform to the far-field assumption made in the echo simulation. The coordinates of each disc were drawn from a uniform random distribution that covered the entire rectangular box. The two-way spreading loss associated with each leaf position created within the rectangular box were tested against the threshold of 80 dB. Leaves in positions with spreading losses that exceed this threshold were discarded, since their contributions to the echo were too small to warrant the computational echoes. Lindenmayer (L-) systems [64] were used to create the inhomogeneous leaf distributions tested here. L-systems are recursive algorithms for creating branching patterns that mimic the growth of biological trees. Each recursion creates an additional level of growth/branching. Two sets of L-system parameters were evaluated in order to create models for two different tree species, eastern white pine and ginkgo. An adult eastern white pine (*Pinus strobus*, Fig 3.1A) was mimicked by an L-system tree model of growth level 13 (Fig 3.1B, gray). The tree model fit into a volume of 2016 m^3 (width, depth, and height: 12, 14, and 12 m). The pine model was based on a bifurcation-type L-system, i.e., two child branches were generated from the tip of each mother branch. Child branches and their mother branches defined a plane that was perpendicular to the plane determined by the mother branch and the branch two growth levels prior to the current branch. The branching angle defines how much the directions of child branches deviate from the direction of their respective mother branch. Since the branching pattern of eastern white pine is monopodial, i.e., there is a single main axis (trunk) to which lateral branches remain subordinate,

one of the two branching angles in each iteration was zero. The other branching angle started at 90° at the first level and decreased by about 5.8° in every higher level until it reached 20° at the 13th level [65] (Fig 3.1B, gray). In each iteration, the length of the child branches became shorter by a constant contraction ratio, which was set to 0.9 for stem branches and 0.7 for side branches. Inspired by real pine trees, thirty 15-cm-long bundles of needles placed spirally around a 4.5-cm-long part of each terminal branch starting from the tip. The branching angle of those bundles was set to 75°. Each bundle was then replaced by five discs placed randomly in a cube with an edge length of 1 cm, the center of which coincided with the tip of the bundle. The orientations of the five discs were defined by vectors between the origin of the bundle and points picked from a uniformly random distribution within the cube. The radial direction of disks were aligned with this vector. The radius lengths of all discs in pine tree were drawn from a Gaussian distribution with a mean of 2 mm and a standard deviation 0.2 mm. For the ginkgo (*Ginkgo biloba*, Fig 3.1D) model, the maximal growth level was set to eight resulting in a volume of 490 m^3 (width, depth, and height: $7\times7\times10$ m, Fig 3.1E, gray). Ginkgo trees have a ternary branching pattern, where three child branches are generated in each branching process: one in the direction of the mother branch, the other two branching off to opposite sides with branching angle of 50°. The contraction ratios were 0.83 for the central branch and 0.62 for each of the two side branches [65]. Four evenly spaced leaf nodes, i.e., short shoots that bear the leaves, were placed on each terminal branch. The leaf nodes divided the terminal branch into four equal parts with one node occupying the tip. Leaf nodes were placed on the non-terminal branches in a similar fashion (even spacing along two opposite sides of the branch, 4 leaves at each node). Leaf nodes placed at the tip of a terminal branch were oriented

in the same direction as the terminal branch; all other leaf nodes were oriented perpendicular to the branch they were placed on. The orientation of first node to be generated was drawn from a uniform random distribution of all orientations perpendicular to the branch. All other nodes were then placed by rotating the orientation of the preceding node by $90°$. The center positions for the leaves belonging to a leaf node on the tip of a terminal branch were selected from a uniform random distribution over a rectangular box ($10\times10\times20$ cm) centered on the node. Leaves from in-branch nodes were displaced from their respective node by a random vector (with all coordinates drawn independently from a uniform distribution) that was added to the vector specifying the direction of the node with a weight of one tenth. The radii of the leaves were drawn from a Gaussian distribution with mean 2.5 cm and standard deviation 0.25 cm.

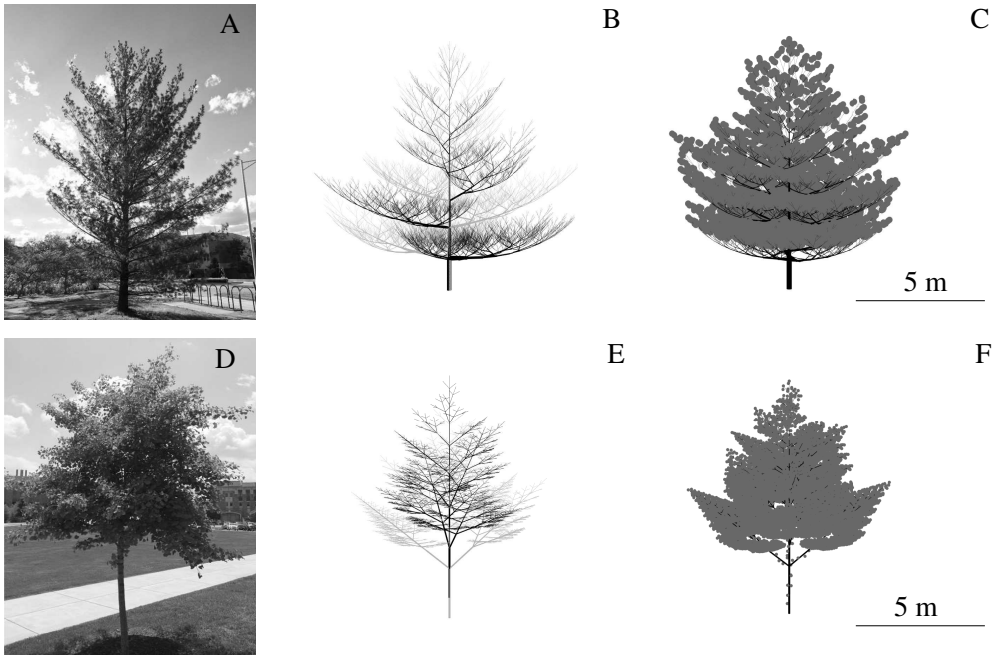

Figure 3.1: Tree specimens with their respective digital tree models constructed using L-systems. A) Eastern white pine (*Pinus strobus*); B) L system model of the same species with its $180°$ rotated version superpositioned to increase the branch density; C) same as B) with leaves added. D),E) and F): same with A), B) and C) for a young ginkgo (*Ginkgo biloba*) except for $90°$'s rotation and that the rotated version is lifted half length of the initial branch along z axis.

Since the tree models that were generated based on the rules described above appeared less dense than natural trees of the same species, a copy of each tree was made by rotating pine and ginkgo $180°$ and $90°$, respectively. The two copies were then added together (Fig 3.1B and E, black). For ginkgo, the copy was also raised by half the length of the initial branch to insure that branches were spaced along the length of the stem.

The beampattern of the simulated sonar was represented by a product of two Gaussian functions, one in elevation and the other in azimuth. For the uniform model, the sonar was always aimed at the foliage. For the uniform leaf distributions as well as the L-system tree models, experiments

with different relative positions and orientations between the biosonar beam and the tree were conducted. Specifically, the following three scenarios were investigated: (i) approach: the sonar was aimed at center of the tree while being translated over distances from 9.5 m down to 2.5 m towards the center of the tree, (ii) angular scan: the aiming direction of the sonar (-3 dB beamwidth 50°, constant target distance about 2 m) is rotated from facing the center of the tree (defined as 0°) to a maximum rotation angle of 90°, and (iii) beam widening: the sonar is kept facing at the center of the tree from a constant distance of about 2 m while the -3 dB two-sided beamwidth is varied between 1° and 60°. To perform matching experiments with the uniform leaf distribution model that can be compared to the results obtained from the L-system tree models, the following adjustments were made to the uniform model: the size of the cuboid leaf domain was adjusted to match the duration of the echoes from the L-system model trees and the uniform leaf density was selected so that the number of leaves in the beam matched those of the L-system model. The leaf size used in uniform-distribution models matched that in L-system models for the two species, respectively. The mean orientation angles for ginkgo and eastern white pine were 45° and 5° with standard deviation 5°, respecitively.

The numerical echo predictions (Fig 3.2B, resulted from scenario Fig 3.2A) for all studied foliage models and sonar-position scenarios were obtained for a frequency band between 60 and 80 kHz which is similar to the second (and strongest) harmonic in the biosonar pulses of the greater horseshoe bat (*Rhinolophus ferrumequinum* [48]). The echoes were simulated by predicting the transfer function for each leaf in this frequency band at 2000 evenly spaced frequencies and complex addition of the individual leaf echoes in the frequency domain. Time-domain signals were derived by

performing an inverse Fourier transform (with a 2000-point Hanning window).

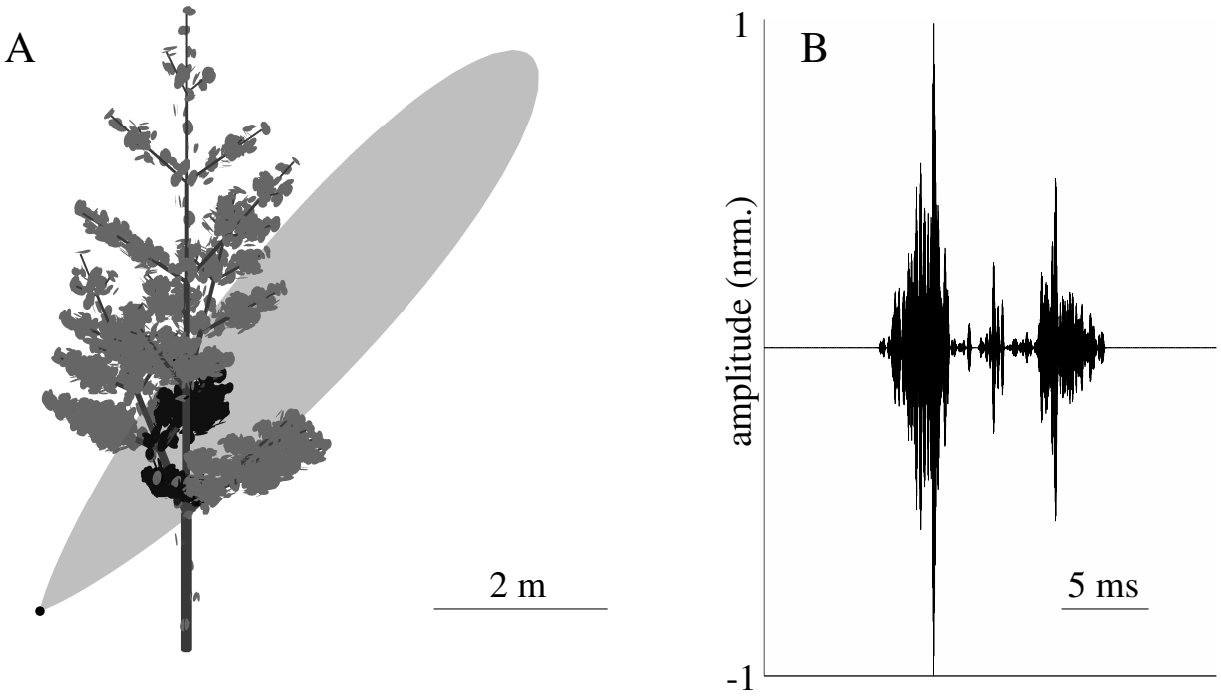

Figure 3.2: Example of a tree model created using an L-system. A) relative position of tree model and simulated sonar beam (sonar position indicated by black dot, -3 dB beamwidth 10°). The leaves with positions within the -3 dB beam contour are colored in black. B) Numerical prediction of impulse response corresponding to the situation depicted in A).

3.3.2 Measure of inhomogeneity

To compare the echoes generated by the uniform leaf-distribution model and the L-system-based models, the hypothesis was investigated that an inhomogeneous distribution of the leaves could give rise to a temporal inhomogeneity in the echoes. To this end, a measure to quantify the inhomogeneity of the echo amplitudes over time was devised as follows: The envelope of each echo was calculated as the magnitude of an analytic signal obtained from the original waveform by virtue of the Hilbert transform [66]. The beginning and the end of the echo were determined by

comparing the envelope amplitudes against a threshold that was set to 100 dB above the numerical noise level defined by the average envelope amplitude away from any simulated echoes. The starting time of the echo was taken to be the time of the first sample that exceeded the threshold and the end was the time of last sample to exceed the threshold. Due to the limited bandwidth of the echo envelopes, the sampling rate of the echo envelope was reduced to 50 kHz from the original 400 kHz that was used for the original echo waveforms. Depending on echo duration, this resulted sample numbers that ranged from a tens of samples up to three thousand samples. Each simulated echo envelope was padded with 50 zeros on each end to ensure that the length of even the shortest echoes was sufficient for the analysis. To gauge inhomogeneity in the echo envelope, the duration of each echo (including the padding) was divided into 100 time windows. A replica of the echo was then created where the time sequence of the 100 windows was randomly permuted. Finally, the root mean square difference between the average amplitudes of the original and the permuted envelopes across all 100 windows was computed as a measure of the temporal inhomogeneity in the echo envelope.

3.3.3 Leaf measurements

Acoustic measurements of leaves were carried out in an anechoic chamber (inner dimensions: $5.4 \times 4.1 \times 2.4$ m). In order to assess the impact of the variability in leaf geometry on target strength an experiment with 100 freshly cut leaves of the leatherleaf arrowwood (*Viburnum rhytidophyllum*) was conducted. For each of the 100 leaves, 50 echoes were measured while the leaf was positioned at a fixing distance of 1.5 m to the sonar. To assess variability across different plant species,

the same measurements were carried out for another nine leaves, each from a different species (Table 3.1). The leaves in the latter experiment were pressed and dry when the measurements were undertaken. The area of each leaf tested was determined from a digital image and used to represent the leaf size by an "equivalent radius", i.e., the radius of the circle with an area equal to the measured area of the leaf.

Table 3.1: Tree species with their respective estimated equivalent leaf radii used in the acoustic leaf characterizations.

Common name	Scientific name	Equivalent radius (cm)
Euonymus, deciduous	*Euonymus alatus*	1.7
Paperbark maple	*Acer griseum*	1.7
River birch	*Betula nigra*	1.8
Ornamental cherry	*Prunus spp.*	1.8
American beech	*Fagus grandifolia*	2.1
Higan cherry	*Prunus subhirtella*	2.5
Redbud	*Cercis canadensis*	2.8
Swamp white oak	*Quercus bicolor*	4.6
Pin oak	*Quercus palustris*	5.0

To assess the impact of shading between leaves, two cardboard disks of radius 1.6 cm were used. The distance between the two discs was varied from 25 cm to 150 cm in increments of 25 cm. The following three measurements were repeated for each distance: First, the distant ("back") disk was ensonified without the other ("front") disk being present. Second, the front disk was placed right along the line of sight from the sonar to the back disk ("fully shaded"). Third, the front disk was displaced to the side by its radius to produce a condition of "partial shading". In all these measurements, the position of the back disk remained fixed. The change of distance between two disks were realized by moving the first disk to a different position at each time.

The impulse responses of leaves and disks were recorded with a biomimetic sonar composed of one electrostatic ultrasonic loudspeaker (Series 600 open face ultrasonic sensor with 4.3 cm diameter, SensComp, Inc., Livonia, MI USA) with a two-sided -6 dB beamwidth of 15°. The loudspeaker was driven by a power amplifier (AA-301HS, A.A. Lab Systems Ltd. Ramat-Gan, Israel). Echo signals were recorded by two MEMS capacitive microphones (SPU0410LR5H, Knowles Electronics, LLC. Itasca, IL USA) integrated on pre-amplifier boards (Momimic, Dodotronic, Rome, Italy). A single A/D&D/A conversion board (NI-6351, National Instruments Corp., Austin, TX, USA) was used to interface the setup with the control computer. Two conical horns (base radius 2.5 cm, top radius 0.25 cm, height 10 cm) were placed in front of microphones. The sonar head was mounted on a tripod which was adjusted to the same height at which the leaves and disks were mounted with thin filament (diameter about 0.3 mm, 12 lb fishing line). The pulse used in the experiments was a periodic pseudo-random sequence (maximum length sequence, MLS, [67]). Each sequence consisted of 255 samples which results in a pulse length of 0.5 ms with the 500 kHz sampling frequency employed.

The maximum value of the recorded impulse responses was determined by fitting a 2nd order polynomial to an 11-point window taken from the envelope of the impulse response in the vicinity of the maximum. The median across all the impulse responses maxima from the 50 echoes that were recorded for each target was used to represent the target's acoustic strength. To compare the predictions from the disk model to the leaf data, a scalar scaling parameter was used to fit the predictions from the model to the measured data in a least-squares sense.

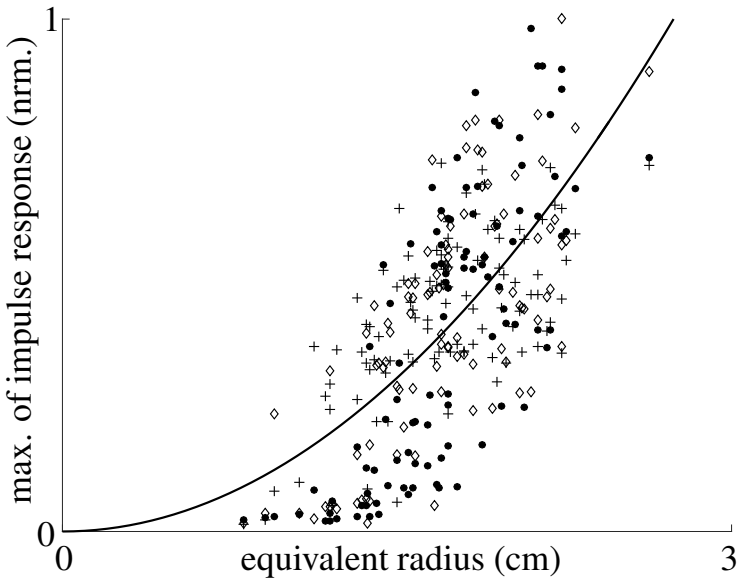

Figure 3.3: Leaf target strength (maximum impulse response amplitude) as a function of equivalent leaf radius. The experimental measurements were obtained for 100 leaf samples from leatherleaf arrowwood (*Viburnum rhytidophyllum*) together with the prediction from the disk model (solid lines). The measurements were repeated three times and each repetition is indicated by a different marker: filled circle (first repetition); diamond (second repetition); plus sign (third repetition); simulation: solid line. 50 echoes were collected for each leaf in each measurement. Each symbol in the plot is the median of 50 impulse response maximums. The fit of the model was accomplished by picking the value of a scalar scaling factor that minimized the deviations between data and model in a least-square sense.

A similar monotonic trend of target strength increasing with equivalent leaf radius was also found across leaves from different species (Fig 3.4). The coefficient of determination was similar to the single-species case (0.58) and the data from the different species seems to fall well within the variation seen in the single-species data set.

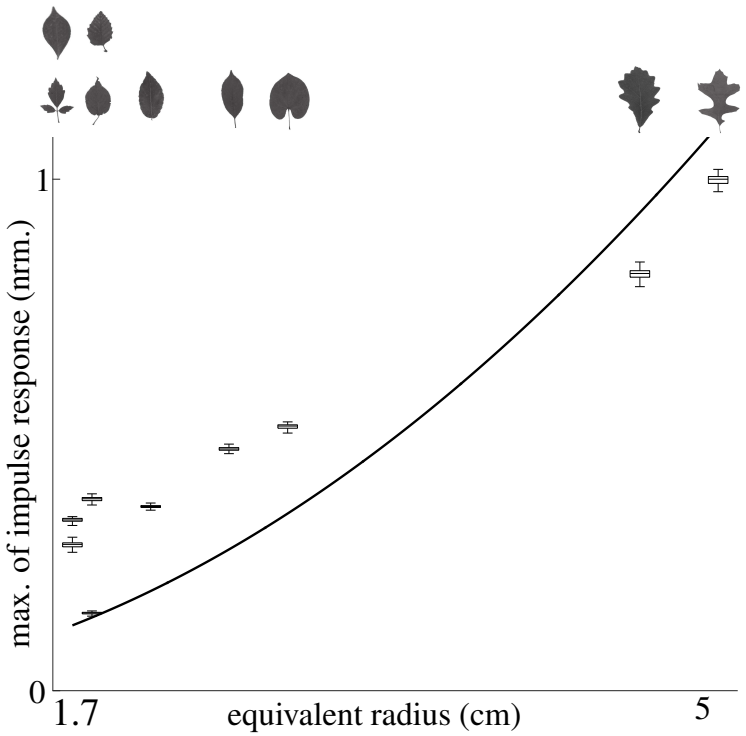

Figure 3.4: Leaf target strength as a function of equivalent radius for individual samples from nine species. The measured values of leaf target strength (maximum impulse response amplitude) are shown together with the predictions from the disc-model (solid line, model fitting as described in Fig 3.3). The silhouettes of the leaves measured are shown in the top of the respective data points.

The acoustic measurements conducted on the disc pairs demonstrated the existence of acoustic shadowing effects between leaves that depended on the distance between the discs (Fig 3.5). At the smallest distance surveyed (25 cm), shading resulted in a drop in target strength of slightly less than 50%, i.e., less than 6 dB. At larger distances, the shadowing effect quickly decreased to reach less than 25% (2.5 dB) at a distance of 75 cm. The differences between the fully shaded and partially shaded conditions were small.

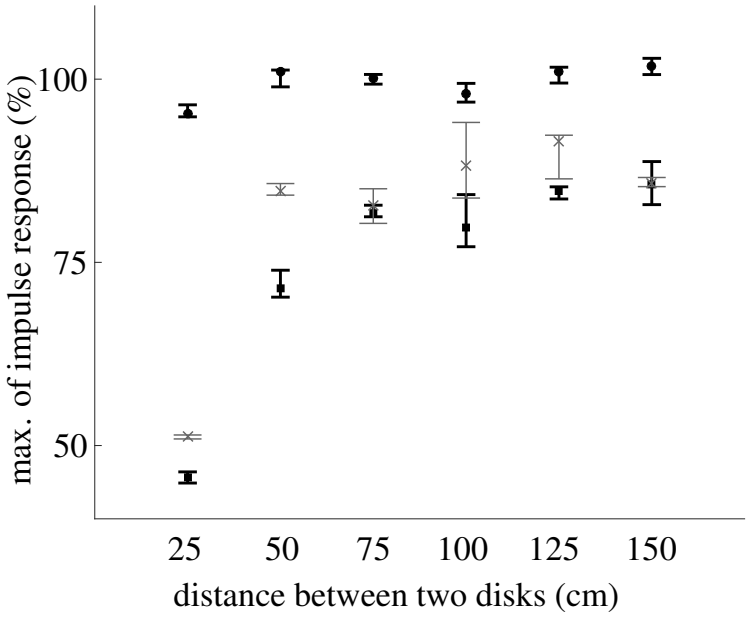

Figure 3.5: Experimental characterization of shading effects between leaves on target strength. Circles: no shading, crosses: complete shading, squares: partially shaded. The diameters of two disks were 3.6 cm. 50 echoes were collected for each situation, the markers represent the mean and the error bars the 75th and 25th percentile of the data set. All amplitude values were normalized with the mean of the impulse response maximums when there was no shading.

The measure of temporal inhomogeneity used here produced non-zero values for all foliage models tested and all relative positions and orientations of the sonar (Fig 3.6). The values of the measure obtained for the uniform leaf distribution model were consistently lower than those that resulted from the two L-system based models for the same experimental condition. However, the differences between the two different model categories were much smaller than the changes that could be elicited by changing the relative position, orientation, or the width of the biosonar beam. Hence, the inhomogeneity measure was found to be far more sensitive to the position and orientation of the sonar relative to the foliage than to the inhomogeneity in the leaf distribution within the foliage.

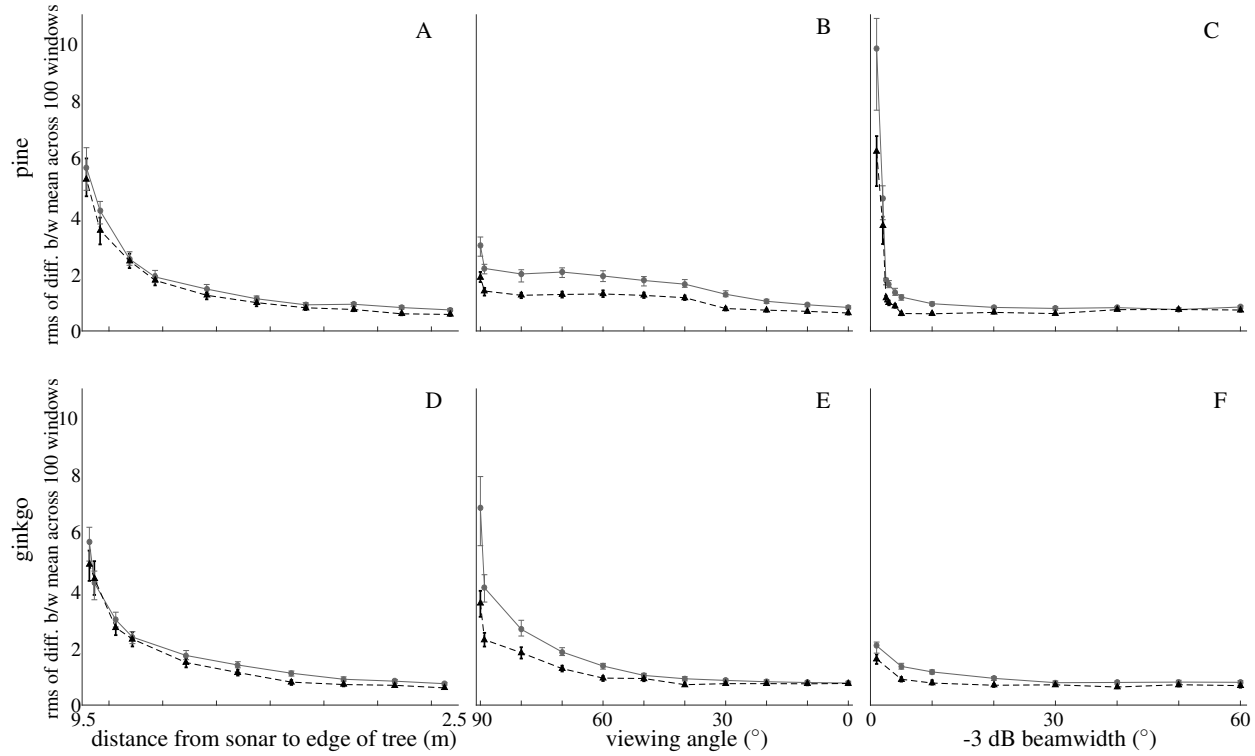

Figure 3.6: Echo envelope inhomogeneity for the L-system tree models compared to a uniform-distribution model reference. Solid lines: L-system tree models, dashed lines: uniform-distribution model. A) and D) Straight approach towards the foliage (A pine, B ginkgo); B) and E) Angular scan with viewing angles ranging from $90°$ to $0°$ (oriented straight at the center, B) pine, E) ginkgo); C) and F) Change in -3 dB beamwidth (C pine, F ginkgo). The leaf density of the uniformly distributed reference models was adjusted in each condition to match the number of leaves in the sonar beam of the two L-system models. In addition, the size of the leaf domain in the uniform leaf distribution model was adjusted to match the echo length in L-systems. Each point represents the mean of 100 experiments, the error bars indicate the minimum and maximum values in each data set.

The three experimental scenarios for changing the sonar position, orientation, and beamwidth in the simulations were each found to have a substantial impact on the temporal inhomogeneity of the echoes (Fig 3.6). As the sonar approached the model foliage, the inhomogeneity decreased monotonically by a factor of approximately six for all three foliage models (Fig 3.6A and D). For the

angular sonar scan, the ratio between the highest and lowest values differed substantially between the pine and the ginkgo model (Fig 3.6B and E). For the pine, the ratio was about three whereas for the ginkgo it was about seven. For both models, the largest values occurred when the sonar was oriented 90 degrees to the side and the smallest values when the sonar was pointed directly at the model foliage. For the changes in beamwidth, all foliage models displayed a decrease in the values of the inhomogeneity measure with increasing beamwidth (Fig 3.6C and F). For the pine model, this decrease was drastic (by a factor of approximately 10) whereas for the ginkgo model it was only by a factor 2.

The direction in which the three experimental conditions impacted the inhomogeneity measure coincides with its impact on the number of leaves that were present in the biosonar beam (Fig 3.7). Whenever large numbers of leaves were in the biosonar beam, the inhomogeneity measure used here showed low values that decreased with an increasing number of leaves being contained in the beam.

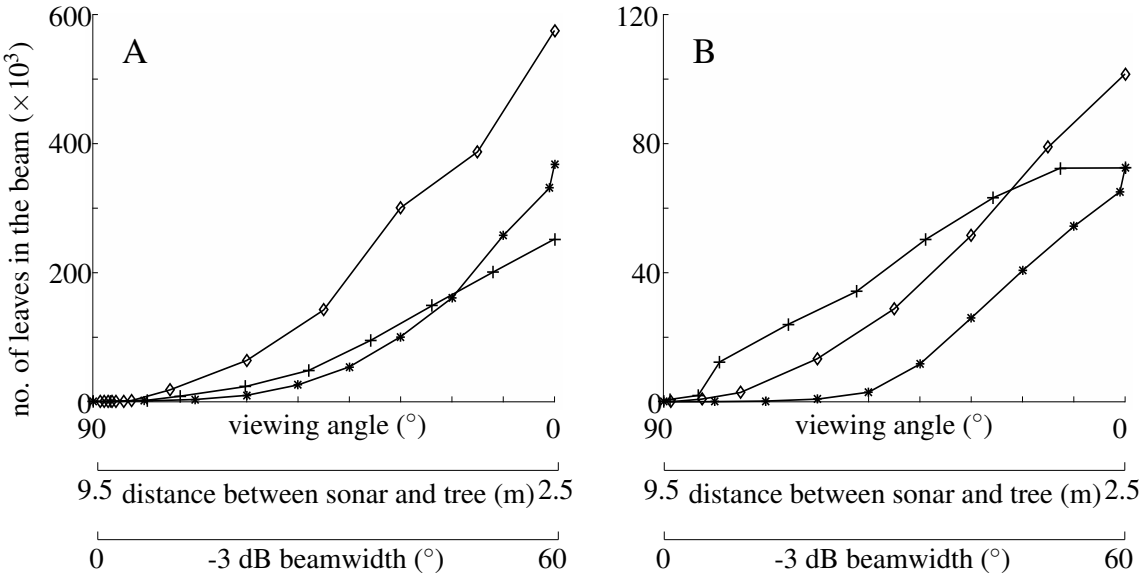

Figure 3.7: Relationship between the pose of the sonar beam and the number of leaves it contains. The number of leaves is given for the volume enclosed by the -80 dB gain surface of the biosonar beam: A) pine, B) ginkgo. Experimental paradigms (Fig 3.6): plus signs: approach; asterisks: rotational scan; diamonds: change in -3 dB beamwidth.

3.4 Discussion

The homogeneous spatial distribution of the leaves in the basic foliage model developed by the authors constitutes an obvious deviation from the situation in natural foliages where the distribution of the leaves is determined by a branching pattern. The results obtained here show a consistently larger temporal inhomogeneity in simulated echoes derived from models with biomimetic branching patterns than in echoes from models with a uniform spatial distribution of the leaves. However, while highly consistent, these differences were also very small compared to the changes in temporal homogeneity seen as a result of varying the relative position of the sonar beam and the foliage. It remains a possibility that spatially inhomogeneous leaf distributions effect the echoes in ways

that are not well represented by the temporal inhomogeneity measure that was introduced and evaluated here. However, if the distribution of the leaves varies along the propagation direction of the pulse, an effect on the echo properties over time seems to be a reasonable expectation. The two tree models that were tested here (ginkgo and pine) were very different in terms of their branching patterns and leaf densities, nevertheless they both have the same consistent results which could be taken as an indication of a general trend. If this is the case, it may not be necessary to sacrifice the simplicity of the uniform leaf distribution to get a reasonable fit to the behavior of natural foliages.

The relationship between temporal inhomogeneity in the echo amplitudes and the relative orientation of the sonar is a highly interesting feature found in the current simulated data set. Since the temporal inhomogeneity was found to be a monotonic function of angle, distance to foliage, and beamwidth, it could be used by the bats to control these properties, e.g., during an angular scan, or derive an estimate of the relative orientation of the sonar beam that could be used as a prior knowledge in the estimation of other foliage properties. This could alleviate, for example, the problem that the authors previously encountered when trying to estimate all three parameters of the simplified foliage model (average leaf size, density, and orientation). If the bat was able to figure out the relative angular orientation of its sonar beam to the foliage surface from the temporal inhomogeneity of the echo envelope, this would allow the animals to predict the orientation of the leaves (assuming the leaf surfaces are oriented in parallel with the foliage surface), leaving only two parameters to be estimated from the echoes.

Differences in geometry (e.g., outline, folding) are a conspicuous feature of natural foliages that is not captured by the simplified numerical foliage model studied here. However, the experimental

results obtained confirm that a simple disk geometry is able to mimic the overall trend in the relationship between leaf size and target strength. The variability in the experimental results can be partially attributed to measurement errors (as evident from the repeated measurements undertaken) and partially to the geometrical complexity of the leaves that is not accounted for by the model. Leaf geometry can hence be seen as an additional factor that increases variability into the echo contributions from individual leaves. It may hence be possible to further improve the current model by using a different probability density function for the leaf size to incorporate this source of variability.

Based on the results obtained here, shadowing effects between the leaves of a foliage could be an important factor in determining the contribution of leaves inside the foliage on the echoes. Leaves in many natural foliage types are frequently spaced less than 25 cm apart and hence could produce substantial shading. It has been reported that echoes from dense and sparse foliages differ in the attenuation of echo amplitudes over time [20]. Hence, it may be possible to adjust the attenuation function in the current model to incorporate the effect of shading between leaves and sonar pulse that penetrates deeper into the foliage. The ideal solution to both issues with the current model (variable leaf geometry and shading) would be based on further insights into how the physical mechanisms can be represented accurately but in a much simpler manner than simulating diffraction by arbitrary leaf geometries and taking into a account the relative positions of the leaves. Future research is needed to establish whether this is possible.

In summary, the physical and modeling experiments carried out here demonstrate that the simple three-parameter model is well suited to approximate natural foliage echoes. Future research should

target improvements that can be made to the model (e.g., addition of a shading function) as well as explore new hypotheses for how the properties of the echoes can be used to support sonar-based navigation in natural environments.

3.5 Acknowledgments

We would like to thank Profs. Ricardo Burdisso, Michael Roan, and Alexander Leonessa for granting the access to the anechoic chamber, Mark Hurtado for help with using the chamber, and Joseph Sutlive for providing training on the data acquisition system used in the experiments.

Chapter 4

Conclusions

4.1 Research accomplishments and findings

The major accomplishments and findings in this work are as follows:

1. A simulation model has been designed and implemented to calculate echoes from foliage by describing the features of a tree with three parameters, mean leaf size, mean orientation, and leaf density. By varying the three parameters, the echoes from a large amount of species can be simulated.

2. The simulated foliage echoes were found to be time-variant. The probability density functions of time windows in the same echo differed from each other. Even if the spreading loss was taken out, the echoes still showed time-varying property. And this property changed to parameters. Bhattacharyya distance, a measure of difference between probability density

functions, increased as the leaf density grew and reduced when the mean leaf orientation was changed gradually from 0°to 90°(from normal incidence to oblique incidence).

3. The foliage parameter estimation experiments have demonstrated that the lasso model can predict one parameter with high accuracy when the other two parameters were known and fixed. When one of the two fixed parameters became variant and unknown, the performance of estimation would be largely reduced.

4. The experiments about leaf geometry showed that the scattering strength was a monotonic function of the leaves' equivalent radii despite of great variability in the acoustic strength of leaves with approximately same sizes. The simulation model was able to follow the relationship between scattering strength and equivalent radius with reasonable accuracy within one species and across species.

5. Shading between two medium disks existed locally, i.e., when one disk was shaded in the direction of sonar's emission by the front disk and the distance between two disks was about 25 cm, the echo received from the shaded disk would be decreased by 50% compared with the case where it was not shaded.

6. Inhomogeneity was found in echoes both from uniform and L-system models, but L-system did contribute more. The inhomogeneity was closely related to the number of leaves in sonar beam.

4.2 Discussion

By approximating leaves as disks, the model is able to include radius and orientation as parameters and thus could describe the beampattern of each individual leaves. The simulation echoes are similar with those recorded from real vegetation, while treating leaves as point reflectors may lead to mimicking only the echoes' temporal statistics [22]. The findings of this work about leaf orientation may help understand bats' orientation behaviors. Echolocating bats tend to use the same flyway (the bundle of many similar individual routes) connecting roosts and hunting areas over many years [17]. Those flyways of bats are usually parallel to linear landscape elements such as tree lines and hedge groves (*M. emarginatus* [68], Mormoopid bats [69]). In other words, bats use landscape elements as guidelines. The orientation of foliage could be an important clue for bats in route-following behaviors. Since it might be hard to measure the orientation of the leaves in real trees, the estimation of it can be conducted with computational tree model where the true orientation value is known. This computational model reduces a tree to three parameters yet can describe the important features of it. It has shown that bats can extract orientation information when they arrive at known habitats (mean leaf size and leaf density are known). If the habitat is unknown to bats, they may fly here and there to figure out the orientation, and then get estimation about the size and density of the leaves, which may later serve as landmarks. Studies have demonstrated that phyllostomid bats have a large capacity for spatial memory [70, 71] and big brown bats (*Eptesicus fuscus*) can rely solely on acoustic echoes from certain landmarks for orientation [18]. By constantly guessing orientation information along with the use of acoustic landmarks and spatial memory, this might enable the bats to follow the same routes for years.

The effective classifications for a single unknown parameter further demonstrate that the observed ability of bats to extract the information contained in vegetation echoes can depend on statistical features [19, 20, 22], since the foliage echoes are typically stochastic superposition of thousands of different reflectors. The features used in this work are typical features that are also accessible to bats, the estimation with which can provide specific information of the trees, such as the orientation and leaf size. This has indicated that echolocating bats are capable of distinguishing a variety of species. Though the lasso model in this work can not estimate multiple unknown parameters well, bats are able to do a much better job with sequential estimation [60]. Also this work discusses the second harmonics of horseshoe bats, fruit-eating bats (*C. perspicillata* and *C. castanea*) exploit more than one harmonics to sense the surroundings [44]. They could alter the frequency of pulse emission and the duration of each pulse in different distance to targets and obstacles. For example, in the terminal phase to the fruit, they could emit very short pulses (0.3–0.5 ms) about 200 times a second to achieve fine localization of the fruit out of the leaves around it. In addition, fruit-eating bats use odor of ripe fruit as a primary cue for detecting food [44]. The comparison between echoes from different harmonics usually enable bats (*Eptesicus fuscus*) to distinguish targets from background clutters [16]. Yet the estimation in this work may provide minimum accessible information for bats from trees. Besides, the frequency range (60 – 80 kHz) here is only 20 kHz, which is on the narrow side of echolocating bats, but can provide good estimation results. So bats with wider frequency range may get more knowledge of the surroundings and the targets than what's presented here.

Real leaves show more variability in acoustic scattering than the leaf model, which may be com-

pensated by adding more variability to leaf radii in the model. Now the leaf radius is drawn from a Gaussian distribution with a mean and standard deviation that's $\frac{1}{10}$ of the mean; however, the standard deviation of the 100 leaves' equivalent radii is $\frac{1}{5}$ of the mean. Besides, the missing variability that lies in the leaves with same equivalent radii might be addressed in the model by multiplying a random number to each disc's beampattern. Compared with leaf geometry, shading has much less impact on the scattering. The lacking effect from shading in the model could also be compensated by increasing the standard deviation of the disk radii. In addition, the L-system may not be required for a simple model, since it doesn't have much influence on the inhomogeneity of the echoes. But when studying bats' behaviors about avoiding obstacles and finding passageways, L-system might be useful. For example, corridors can be constructed by trimming several branches or putting several trees together with different spacings, while it may not make much sense to find corridors with uniform model especially when the leaf density is very high. At that time, inhomogeneity in echoes could be a clue for bats about how their beams are oriented to the tree and also the relative position to the tree, since the results show that inhomogeneity changes to the relative spatial position of bats to the tree regardless of tree species.

4.3 Suggestions for future work

1. The "holes" and/or "corridors" can be simulated with branching patterns from L-system incorporated with the leaf model. Hence, study of how echolocating bats find passageways according to their echoes can be investigated by simulation.

2. The model with L-system may be exploited to study the contour-following behaviors of the bats by placing the sonar along the edge of the tree and moving it forward. Possible cues for bats might be found in the echoes.

3. The echoes of real bats might be collected from the foliage. The lasso model might be tested in estimating leaf size at least, since it's hard in practice to evaluate the true density and orientation. But leaf size is relatively easier to know by measuring leaf specimens.

Bibliography

[1] C. Sanchez, H. Arribart, and M.M.G. Guille. Biomimetism and bioinspiration as tools for the design of innovative materials and systems. *Nat. Mater.*, 4(4):277–288, 2005.

[2] W. Barthlott and C. Neinhuis. Purity of the sacred lotus, or escape from contamination in biological surfaces. *Planta*, 202(1):1–8, 1997.

[3] B. Karthick and R. Maheshwari. Lotus-inspired nanotechnology applications. *Resonance*, 13(12), 2008.

[4] D. D. Cox and T. Dean. Neural networks and neuroscience-inspired computer vision. *Curr. Biol.*, 24(18):R921–R929, 2014.

[5] Y. Bar-Cohen. Biomimetics – using nature to inspire human innovation. *Bioinspir. Biomim.*, 1(1):P1, 2006.

[6] D. R. Griffin. *Listening in the Dark*. Yale University Press, New Haven, CT, 1st edition, 1958.

[7] J. Fullard and J. Dawson. The echolocation calls of the spotted bat *Euderma maculatum* are relatively inaudible to moths. *J. Exp. Biol.*, 200(1):129–137, 1997.

[8] M. B. Fenton and G. P. Bell. Recognition of species of insectivorous bats by their echolocation calls. *J. Mammal.*, 62(2):233–243, 1981.

[9] A. D. Grinnell and D. R. Griffin. The sensitivity of echolocation in bats. *Biol. Bull.*, 114(1):10–22, 1958.

[10] Y. Gustafson and H. U. Schnitzler. Echolocation and obstacle avoidance in the hipposiderid bat *Asellia tridens*. *J. Comp. Physiol.*, 131(2):161–167, 1979.

[11] E. L. Anthony and T. H. Kunz. Feeding strategies of the little brown bat, *Myotis lucifugus*, in southern new hampshire. *Ecology*, 58(4):775–786, 1977.

[12] J. Müller and W. Burgard. Efficient probabilistic localization for autonomous indoor airships using sonar, air flow, and IMU sensors. *Adv. Robot.*, 27(9):711–724, 2013.

[13] J. Müller, A. Rottmann, L. M. Reindl, and W. Burgard. A probabilistic sonar sensor model for robust localization of a small-size blimp in indoor environments using a particle filter. In *IEEE Int. Conf. Robot. Autom.*, pages 3589–3594, 2009.

[14] A.J. Barry and R. Tedrake. Pushbroom stereo for high-speed navigation in cluttered environments. *IEEE Int. Conf. Robot. Autom.*, pages 3046–3052, 2015.

[15] B. Landry, R. Deits, P. R. Florence, and R. Tedrake. Aggressive quadrotor flight through

cluttered environments using mixed integer programming. In *IEEE Int. Conf. Robot. Autom.*, pages 1469–1475, 2016.

[16] M. E. Bates, J. A. Simmons, and T. V. Zorikov. Bats use echo harmonic structure to distinguish their targets from background clutter. *Science*, 333(6042):627–630, 2011.

[17] A. Schaub and H.U. Schnitzler. Flight and echolocation behaviour of three vespertilionid bat species while commuting on flyways. *J. Comp. Physiol. A*, 193(12):1185–1194, 2007.

[18] M. E. Jensen, C. F. Moss, and A. Surlykke. Echolocating bats can use acoustic landmarks for spatial orientation. *J. Exp. Biol.*, 208(23):4399–4410, 2005.

[19] J.E. Grunwald, S. Schörnich, and L. Wiegrebe. Classification of natural textures in echolocation. *Proc. Natl. Acad. Sci. U.S.A.*, 101(15):5670–5674, 2004.

[20] R. Müller and R. Kuc. Foliage echoes: a probe into the ecological acoustics of bat echolocation. *J. Acoust. Soc. Am.*, 108(2):836–845, 2000.

[21] R. Müller. A computational theory for the classification of natural biosonar targets based on a spike code. *Network*, 14(3):595–612, 2003.

[22] Y. Yovel, P. Stilz, M. O. Franz, A. Boonman, and H. U. Schnitzler. What a plant sounds like: the statistics of vegetation echoes as received by echolocating bats. *PLoS Comput. Biol.*, 5(7):e1000429, 2009.

[23] Y. Yovel, M.O. Franz, P. Stilz, and H. U. Schnitzler. Plant classification from bat-like echolocation signals. *PLoS Comput. Biol.*, 4(3):e1000032, 2008.

[24] J.R. Rosell and R. Sanz. A review of methods and applications of the geometric characterization of tree crops in agricultural activities. *Comput. Electron. Agric.*, 81:124–141, 2012.

[25] H. Li, C. Zhai, P. Weckler, N. Wang, S. Yang, and B. Zhang. A canopy density model for planar orchard target detection based on ultrasonic sensors. *Sensors*, 17(1):31, 2016.

[26] P. McKerrow and N. Harper. Plant acoustic density profile model of CTFM ultrasonic sensing. *IEEE Sensors J.*, 1(4):245–255, 2001.

[27] A.W. Schumann and Q.U. Zaman. Software development for real-time ultrasonic mapping of tree canopy size. *Comput. Electron. Agric.*, 47(1):25–40, 2005.

[28] J. Llorens, E. Gil, J. Llop, and A. Escolà. Ultrasonic and LIDAR sensors for electronic canopy characterization in vineyards: Advances to improve pesticide application methods. *Sensors*, 11(2):2177–2194, 2011.

[29] H. Maghsoudi, S. Minaei, B. Ghobadian, and H. Masoudi. Ultrasonic sensing of pistachio canopy for low-volume precision spraying. *Comput. Electron. Agric.*, 112:149–160, 2015.

[30] V. Jejčič, T. Godeša, M. Hočevar, B. Širok, A. Malneršič, A. Štancar, M. Lešnik, and D. Stajnko. Design and testing of an ultrasound system for targeted spraying in orchards. *Stroj. Vestnik J. Mech. Eng.*, 57(7-8):587–598, 2011.

[31] D. Stajnko, P. Berk, M. Lešnik, V. Jejčič, M. Lakota, A. Štrancar, M. Hočevar, and J. Rakun. Programmable ultrasonic sensing system for targeted spraying in orchards. *Sensors*, 12(11):15500–15519, 2012.

[32] E. Gil, A. Escolà, J.R. Rosell, S. Planas, and L. Val. Variable rate application of plant protection products in vineyard using ultrasonic sensors. *Crop Prot.*, 26(8):1287–1297, 2007.

[33] P. Balsari, G. Pergher, G. Ade, M. Vier, P. Guarella, G. Glametta, and E. Cerruto. The usefulness of a test area for the calibration of sprayer for grapevines. *Inf. Agrar*, 58:97–108, 2002.

[34] A. Escolà, J.R. Rosell-Polo, S. Planas, E. Gil, J. Pomar, F. Camp, J. Llorens, and F. Solanelles. Variable rate sprayer. Part 1–Orchard prototype: design, implementation and validation. *Comput. Electron. Agric.*, 95:122–135, 2013.

[35] P.J. Walklate, J.V. Cross, G.M. Richardson, R.A. Murray, and D.E. Baker. It–Information technology and the human interface: Comparison of different spray volume deposition models using LIDAR measurements of apple orchards. *Biosyst. Eng.*, 82(3):253–267, 2002.

[36] S.D. Tumbo, M. Salyani, J.D. Whitney, T.A. Wheaton, and W.M. Miller. Investigation of laser and ultrasonic ranging sensors for measurements of citrus canopy volume. *Appl. Eng. Agric.*, 18(3):367, 2002.

[37] Q.U. Zaman and M. Salyani. Effects of foliage density and ground speed on ultrasonic measurement of citrus tree volume. *Appl. Eng. Agric.*, 20(2):173, 2004.

[38] A.W. Schumann, W.M. Miller, Q.U. Zaman, K.H. Hostler, S. Buchanon, and S. Cugati. Variable rate granular fertilization of citrus groves: Spreader performance with single-tree prescription zones. *Appl. Eng. Agric.*, 22(1):19–24, 2006.

[39] J.L. Gamarra-Diezma, A. Miranda-Fuentes, J. Llorens, A. Cuenca, G. L. Blanco-Roldán, and A. Rodríguez-Lizana. Testing accuracy of long-range ultrasonic sensors for olive tree canopy measurements. *Sensors*, 15(2):2902–2919, 2015.

[40] H.U. Schnitzler, C. F. Moss, and A. Denzinger. From spatial orientation to food acquisition in echolocating bats. *Trends Ecol. Evol.*, 18(8):386–394, 2003.

[41] J.A. Simmons. The resolution of target range by echolocating bats. *J. Acoust. Soc. Am.*, 54(1):157–173, 1973.

[42] H. U. Schnitzler and E. K. V. Kalko. Echolocation by insect-eating bats. *BioScience*, 51(7):557–569, 2001.

[43] D. von Helversen and O. von Helversen. Acoustic guide in bat-pollinated flower. *Nature*, 398(6730):759–760, 1999.

[44] W. Thies, E.K.V. Kalko, and H.U. Schnitzler. The roles of echolocation and olfaction in two neotropical fruit-eating bats, *Carollia perspicillata* and *C. castanea*, feeding on *Piper*. *Behav. Ecol. Sociobiol.*, 42(6):397–409, 1998.

[45] R. Simon, M.W. Holderied, C.U. Koch, and O. von Helversen. Floral acoustics: conspicuous echoes of a dish-shaped leaf attract bat pollinators. *Science*, 333(6042):631–633, 2011.

[46] D. Genzel and L. Wiegrebe. Size does not matter: size-invariant echo-acoustic object classification. *J. Comp. Physiol. A*, 199(2):159–168, 2013.

[47] J. J. Bowman, T. B. Senior, and P. L. Uslenghi. *Electromagnetic and acoustic scattering by simple shapes*. Hemisphere Publishing Corp., New York, revised edition, 1987.

[48] M. M. Andrews and P. T. Andrews. Ultrasound social calls made by greater horseshoe bats (*Rhinolophus ferrumequinum*) in a nursery roost. *Acta Chiropt.*, 5(2):221–234, 2003.

[49] R. Adelman, N. A. Gumerov, and R. Duraiswami. Software for computing the spheroidal wave functions using arbitrary precision arithmetic. *arXiv preprint*, arXiv:1408.0074, 2014.

[50] T. F. Coleman and Y. Li. An interior trust region approach for nonlinear minimization subject to bounds. *SIAM J. Optimiz.*, 6(2):418–445, 1996.

[51] H.U. Schnitzler and A.D. Grinnell. Directional sensitivity of echolocation in the horseshoe bat, *Rhinolophus ferrumequinum*. *J. Comp. Physiol.*, 116(1):63–76, 1977.

[52] G. R. Long and H. U. Schnitzler. Behavioural audiograms from the bat, *Rhinolophus ferrumequinum*. *J. Comp. Physiol.*, 100(3):211–219, 1975.

[53] M.F. Robinson. A relationship between echolocation calls and noseleaf widths in bats of the genera *Rhinolophus* and *Hipposideros*. *J. Zool.*, 239(2):389–393, 1996.

[54] H. Zhao, S. Zhang, M. Zuo, and J. Zhou. Correlations between call frequency and ear length in bats belonging to the families Rhinolophidae and Hipposideridae. *J. Zool.*, 259(2):189–195, 2003.

[55] R. Tibshirani. Regression shrinkage and selection via the lasso. *J. R. Stat. Soc. Series B (Methodological)*, pages 267–288, 1996.

[56] C. Q. Tang and M. Ohsawa. Altitudinal distribution of evergreen broad-leaved trees and their leaf-size pattern on a humid subtropical mountain, Mt. Emei, Sichuan, China. *Plant Ecol.*, 145(2):221–233, 1999.

[57] A. Bhattachayya. On a measure of divergence between two statistical population defined by their population distributions. *Bull. Calcutta Math. Soc.*, 35(99-109):28, 1943.

[58] F.J. Massey Jr. The Kolmogorov–Smirnov test for goodness of fit. *JASA*, 46(253):68–78, 1951.

[59] J. A. Simmons, W. A. Lavender, B. A. Lavender, C. A. Doroshow, S. W. Kiefer, R. Livingston, A. C. Scallet, and D. E. Crowley. Target structure and echo spectral discrimination by echolocating bats. *Science*, 186(4169):1130–1132, 1974.

[60] R. Kuc. Transforming echoes into pseudo-action potentials for classifying plants. *J. Acoust. Soc. Am.*, 110(4):2198–2206, 2001.

[61] R. Kuc. Neuro-computational processing of moving sonar echoes classifies and localizes foliage. *J. Acoust. Soc. Am.*, 116(3):1811–1818, 2004.

[62] C. Ming, A. K. Gupta, R. Lu, H. Zhu, and R. Müller. A computational model for biosonar echoes from foliage. *PLoS ONE*, 12(8):e0182824, 2017.

[63] J.A. Stratton. *Electromagnetic theory*. John Wiley & Sons, 2007.

[64] A. Lindenmayer. Mathematical models for cellular interactions in development I. Filaments with one-sided inputs. *J. Theor. Biol.*, 18(3):280–299, 1968.

[65] M. Aono and T. L. Kunii. Botanical tree image generation. *IEEE Comput. Graph. Appl.*, 4(5):10–34, 1984.

[66] L. Marple. Computing the discrete-time "analytic" signal via FFT. *IEEE Trans. Signal Process.*, 47(9):2600–2603, 1999.

[67] M.R. Schroeder. Integrated-impulse method measuring sound decay without using impulses. *J. Acoust. Soc. Am.*, 66(2):497–500, 1979.

[68] D. Krull, A. Schumm, W. Metzner, and G. Neuweiler. Foraging areas and foraging behavior in the notch-eared bat, *Myotis emarginatus* (Vespertilionidae). *Behav. Ecol. Sociobiol.*, 28(4):247–253, 1991.

[69] G. C. Bateman and T. A. Vaughan. Nightly activities of mormoopid bats. *J. Mammal.*, 55(1):45–65, 1974.

[70] D. von Helversen and O. von Helversen. Object recognition by echolocation: a nectar-feeding bat exploiting the flowers of a rain forest vine. *J. Comp. Physiol. A*, 189(5):327–336, 2003.

[71] Y. Winter and K. P. Stich. Foraging in a complex naturalistic environment: capacity of spatial working memory in flower bats. *J. Exp. Biol.*, 208(3):539–548, 2005.

Appendix A

Program Source

A.1 to A.10 are programs developed to calculate the foliage echoes in Chapter 2. The program named Sim_leaf_scattering.m can be run to get echoes after entering the values of three parameters, leaf density, mean leaf radius, and average orientation, names of which in the script are leafdensity, leafsize, and alphax, respectively. Other scripts are functions called by Sim_leaf_scattering.m or by functions in it.

A.1 Sim_leaf_scattering.m

This program is the main code to run to record echoes. Programs after this are subfunctions which support Sim_leaf_scattering.m.

```
%%% Sim scattering: Run the leaf scattering simulation and record echoes
%Created by: Anupam Kumar Gupta, Date:09/01/2015, Modified by Chen Ming,
%Date: 10/01/2015

%%% Support for volume within which leaves are distributed uniformally
pos_param.bound = [1 10;-2 2;-2 2];% x,y,z-axes support (bounding box
    dimensions, meters)

%%% Leaf distribution parameters

leafdensity = 50; % number of leaves per cubic meter, N/m^3
leafsize = 2E-2; % mean leaf radius, m
alphax = 45; % mean leaf orientation, in degrees
```

```
leaf_param.leafsize_dist = 'gauss'; % can choose from 'uni' (uniform) and '
    gauss' (Gaussian), but leafsize_supp has to be [upper, lower] limit
leaf_param.leafsize_supp = []; % leaf radius range in m, single value for '
    gauss', [a,b] form for 'uni'
% the angle between x axis and leaf normal vector in degrees

%%% Sonar parameters
sonar_param.loc = [0 0 0];
sonar_param.peakAmp = 1;% Peak amplitude of sonar beampattern
sonar_param.freqorbmwdth = 'beamwidth';
sonar_param.freqorbmwdthVal = 30;% beamwidth in degrees (elevation and azimuth
     same)
sonar_param.beamcenter = [0 0];% beam center coordinates
sonar_param.noise = [];

%%% Echo parameters
n_echoes = 1;  % no of echoes to generate per paramater combination
echo_param.n_echoes = n_echoes;
echo_param.Gthresh = 20; % gain value for thresholding (dB)
echo_param.Fs = 400; % sampling frequency (kHz)
echo_param.Nbins = 24E3; % no of bins b/w 60-80 kHz

s = zeros(n_echoes, echo_param.Nbins); % the impulse responses
for i = 1:n_echoes
                leaf_param.density = leafdensity;
                leaf_param.leafsize_supp = leafsize;
                [Sphcoord_sonar,Sphcoord_leaf,Sphcoord_leafnorm,leaf_dia] =
                    leaf_dist_uniform1(pos_param,leaf_param,sonar_param,alphax
                    );
                [~,~,R_sonar_leaf_filt,leaf_dia_filt,Sonargain_filt,
                    Incident_angles] = filter_leaves_beamG(echo_param,
                    Sphcoord_sonar,Sphcoord_leaf,Sphcoord_leafnorm,leaf_dia,
                    sonar_param);
                s(i,:) = time_domain_impulse1(Sonargain_filt,R_sonar_leaf_filt
                    ,leaf_dia_filt,Incident_angles,echo_param);
end
```

A.2 leaf_dist_uniform1.m

This program creates uniformly distributed leaf locations and samples leaf sizes and orientations from two normal distributions.

```
function [Sphcoord_sonar,Sphcoord_leaf,Sphcoord_leafnorm,leaf_dia] =
    leaf_dist_uniform1(pos_param,leaf_param,sonar_param, alphax)
%LEAF_DIST_UNIFORM: Draws the leaf locations from a uniform distribution &
%returns the sonar,leaf centers,leaf normal spherical coordinates, leaf
%diameters, distance/range between sonar and leaf.
% Inputs:
```

```
%        pos_param, the struct contains the info of leaf locations.
%        pos_param.bound: x,y,z-axes support (bounding box dimensions, meters)
%
%        leaf_param, the struct contains the info about the distribution of
%        leaves
%        leaf_param.
%            leafloc_dist, the distribution of leaf locations
%            leafsize_dist, the distribution of leaf radii
%            leafsize_supp, the leaf radius support for uniform distribution
%
%        sonar_param, the struct contains the info about sonar, details of
%        each field please see comments in Sim_leaf_scattering.m
%        alphax, the mean leaf orientation angle, standard deviation: 5
%        degrees
% Outputs:
%         TH_sonar (Azimuth),PHI_sonar (Elevation),R_sonar (Range): Spherical
   coordinates of sonar in radians, Sphcoord_sonar.
%         TH_leaf,PHI_leaf,R_leaf: Spherical coordinates of leaf centers in
%             radians, Sphcoord_leaf.
%         TH_leaf_norm,PHI_leaf_norm: Spherical coordinates of leaf normals
%             in radians, Sphcoord_leafnorm.
%         leaf_dia: Vector containing leaf diameters in meters.
%Created by:Anupam Kumar Gupta,Date: 1/12/2015, Modified by Chen Ming, Date
%10/01/2015


%%% Bounding Box params
ax = pos_param.bound(1,1);
bx = pos_param.bound(1,2);
ay = pos_param.bound(2,1);
by = pos_param.bound(2,2);
az = pos_param.bound(3,1);
bz = pos_param.bound(3,2);
%%% Leaf params
leaf_density = leaf_param.density;
leaf_size_dist = leaf_param.leafsize_dist;
mleaf_size = leaf_param.leafsize_supp;

%%% Sonar params
sonar_loc = sonar_param.loc;

%%% Find number of leaf  from the envelope volume and leaf density
Env_vol = (bx-ax)*(by-ay)*(bz-az);
n_leaf = round(Env_vol * leaf_density);


%%% Leaf locations:Uniform or Gaussian

        xleafloc = random('Uniform',ax,bx,n_leaf,1);
        yleafloc = random('Uniform',ay,by,n_leaf,1);
        zleafloc = random('Uniform',az,bz,n_leaf,1);
```

```
%%% Generate the leaf sizes (radius)

switch leaf_size_dist
    case 'uni'

        % Generate the leaf sizes from a uniform distribution

        % parameters for uniform distribution

        if (length(leaf_size_sup) == 2)
            a_leaf = leaf_size_sup(1);
            b_leaf = leaf_size_sup(2);
        else
            error('Wrong input');
        end

        leaf_dia = random('Uniform',a_leaf,b_leaf,n_leaf,1);

    case 'gauss'

        %%% Generate the leaf sizes from a gaussian distribution

        % parameters for normal distribution

            leaf_rds_mean = mleaf_size;
            leaf_rds_sigma = 0.1*mleaf_size;

          pd = makedist('Normal','mu',leaf_rds_mean,'sigma',leaf_rds_sigma);
          tr = truncate(pd,0,1);
          leaf_dia = random(tr, n_leaf,1);
end

%%% Sonar location
if (length(sonar_loc) == 3)

    x_sonar = sonar_loc(1);
    y_sonar = sonar_loc(2);
    z_sonar = sonar_loc(3);
else
    error('Wrong input');
end

%%% Translate the coordinate system origin to sonar center
x_sonartrans = x_sonar - x_sonar;
y_sonartrans = y_sonar - y_sonar;
z_sonartrans = z_sonar - z_sonar;

LeafcenM = [xleafloc(:) yleafloc(:) zleafloc(:)];
Transmatrix = repmat([-x_sonar -y_sonar -z_sonar],n_leaf,1);
Leafcentrans = LeafcenM+Transmatrix; % Transmatrix is 0 matrix here.
```

```
% Convert the leaf, leaf surface normals & sonar coordinates from cartesian to
    spherical
[TH_leaf_sonar,PHI_leaf_sonar,R_leaf_sonar] = cart2sph([Leafcentrans(:,1);
   x_sonartrans],[Leafcentrans(:,2);y_sonartrans],[Leafcentrans(:,3);
   z_sonartrans]);


%%% Leaf
TH_leaf = TH_leaf_sonar(1:end-1);
PHI_leaf = PHI_leaf_sonar(1:end-1);
R_leaf = R_leaf_sonar(1:end-1);

%%% Leaf normal vectors
mu = alphax;
sigma = 5; % the std of the angle between pulse direction and leaf normal
   vector, in degrees
pd_alpha = makedist('Normal','mu',mu,'sigma',sigma);
tr_alpha = truncate(pd_alpha,0,90);
alpha_deg = random(tr_alpha,n_leaf,1);
alpha_rad = deg2rad(alpha_deg);

theta = 2*pi*rand(n_leaf,1);
X = ones(n_leaf,1);
Y = tan(alpha_rad).*sin(theta);
Z = tan(alpha_rad).*cos(theta);

[TH_leaf_norm, PHI_leaf_norm, ~] = cart2sph(X,Y,Z);

R_leaf_norm = ones(n_leaf,1);
%%% Sonar
TH_sonar = TH_leaf_sonar(end);
PHI_sonar = PHI_leaf_sonar(end);
R_sonar = R_leaf_sonar(end);

%%% Outputs
Sphcoord_leaf= [TH_leaf(:) PHI_leaf(:) R_leaf(:)];
Sphcoord_leafnorm.TH_leaf_norm = TH_leaf_norm;
Sphcoord_leafnorm.PHI_leaf_norm = PHI_leaf_norm;
Sphcoord_leafnorm.R_leaf_norm = R_leaf_norm;
Sphcoord_sonar = [TH_sonar PHI_sonar R_sonar];

end
```

A.3 filter_leaves_beamG.m

This function is to filter leaves that are outside of the thresholded iso-surface of the sonar beam, and calculate the incident angles of each leaf.

```
function [Sphcoord_leaf_filt,Sphcoord_leafnorm_filt,R_sonar_leaf_filt,
    leaf_dia_filt,Sonargain_filt,Incident_angles] = filter_leaves_beamG(
    echo_param,Sphcoord_sonar,Sphcoord_leaf,Sphcoord_leafnorm,leaf_dia,
    sonar_param)
% Filter_Leaves_BeamG: Takes in the uniformly distributed leaf locations in
% a box and filters them based on a incoming (sonar) amplitude threshold
% Inputs: (Before gain based filtering)
%        TH_sonar (Azimuth),PHI_sonar (Elevation),R_sonar (Range): Spherical
    coordinates of sonar in radians, Sphcoord_sonar.
%        TH_leaf,PHI_leaf,R_leaf: Spherical coordinates of leaf centers in
%            radians, Sphcoord_leaf.
%        TH_leaf_norm,PHI_leaf_norm: Spherical coordinates of leaf normals
%            in radians, Sphcoord_leafnorm.
%        leaf_dia: Vector containing leaf diameters in meters.
%        echo_param: General information about echo, details please see
%        Sim_leaf_scattering.m
%
%        freqorbmwdth: 1) 'incident_freq' for entering frequency of incidence
%        b/w 60-80 kHz in kHz to estimate spread(sigma) of gauss beampattern
%        based on horseshoe data, 2) 'beamwidth' for directly entering
%        beamwidth in degrees and estimate spread(sigma) of gauss
%        beampattern for the same
%        freqorbmwdthVal: frequency (kHz) b/w 60-80 kHz for 'incident_freq' in
     freqorbmwdth
%        and beamwidth (degrees) for 'beamwidth' in freqorbmwdth.
%
% Outputs: (After gain based filtering)
%        TH_sonar (Azimuth),PHI_sonar (Elevation),R_sonar (Range): Spherical
    coordinates of sonar in radians.
%        TH_leaf_filt,PHI_leaf_filt,R_leaf_filt: Spherical coordinates of leaf
     centers in
%            radians.
%        TH_leaf_norm,PHI_leaf_norm: Spherical coordinates of leaf normals
%            in radians.
%        leaf_dia_filt: Vector containing leaf diameters in meters.
%        Sonargain_filt: Vector containing sonar amplitude/gain at each leaf
% Created by: Anupam Kumar Gupta, Date:08/27/2015, Modified by Chen Ming,
% Date 11/01/2015

%%% Sonar params
TH_sonar = Sphcoord_sonar(1);
PHI_sonar = Sphcoord_sonar(2);
R_sonar = Sphcoord_sonar(3);
Sonaramp = sonar_param.peakAmp;
freqorbmwdth = sonar_param.freqorbmwdth;
```

```
freqorbmwdthVal = sonar_param.freqorbmwdthVal;
beamcenter = sonar_param.beamcenter;

%%% Leaf params
TH_leaf = Sphcoord_leaf(:,1);
PHI_leaf = Sphcoord_leaf(:,2);
R_leaf = Sphcoord_leaf(:,3);

%%% Leaf normal params
TH_leaf_norm = Sphcoord_leafnorm.TH_leaf_norm;
PHI_leaf_norm = Sphcoord_leafnorm.PHI_leaf_norm;
R_leaf_norm = Sphcoord_leafnorm.R_leaf_norm;

%%%% Find relative location of sonar w.r.t leaves and vice versa

%%% Relative distance between leaf center and sonar (range)

R_sonar_leaf = dist_points_sph_coord(R_leaf,TH_leaf,PHI_leaf,R_sonar*ones(size
    (R_leaf)),TH_sonar*ones(size(TH_leaf)),PHI_sonar*ones(size(PHI_leaf)));

%%% Angle between leaf center and sonar center
Az_sonar_leaf = TH_sonar - TH_leaf;
El_sonar_leaf = PHI_sonar - PHI_leaf;

%%% Filter leaves based on beam gain
Zgain_sonar_emission = gauss_beam_sonar(Sonaramp,freqorbmwdth,freqorbmwdthVal,
    beamcenter,sonar_param.noise);

Zgain_sonar = Zgain_sonar_emission.^2; % Here, counting for the reception
    beampattern.
el = linspace(-pi/2,pi/2,181); % elevation
az = linspace(-pi,pi,361); % azimuth

%%% Sonar beampattern gain
[~,elloc_sonar] = min(abs(bsxfun(@minus,El_sonar_leaf,el)),[],2);
[~,azloc_sonar] = min(abs(bsxfun(@minus,Az_sonar_leaf,az)),[],2);
idx = sub2ind(size(Zgain_sonar),elloc_sonar,azloc_sonar);
sonarbp_gain = Zgain_sonar(idx); % sonar gain


p_ref = 2*1E-5; % reference sound pressure in air, in pascal
p0 = 2; % in pascal
r0 = 0.1; % in m, reference distance.

dis_b2 = r0^2*p0*sonarbp_gain/10^(echo_param.Gthresh/20)/p_ref;
dis_b = sqrt(dis_b2);
idxfilter = find(R_sonar_leaf <= dis_b); %find the index where gain is greater
     than threshold

%%% Extract leaves & parameters that pass gain threshld
TH_leaf_filt = TH_leaf(idxfilter);
```

```
PHI_leaf_filt = PHI_leaf(idxfilter);
R_leaf_filt = R_leaf(idxfilter);


TH_leaf_norm_filt = TH_leaf_norm(idxfilter,:);
PHI_leaf_norm_filt = PHI_leaf_norm(idxfilter,:);
R_leaf_norm_filt = R_leaf_norm(idxfilter,:);

leaf_dia_filt = leaf_dia(idxfilter);
R_sonar_leaf_filt = R_sonar_leaf(idxfilter);

Sonargain_filt = sonarbp_gain(idxfilter);

%%% Angle between leaf axis and leaf normal
Vec1 = [R_sonar*ones(size(R_leaf_filt)) TH_sonar*ones(size(TH_leaf_filt))
    PHI_sonar*ones(size(PHI_leaf_filt)) R_leaf_filt TH_leaf_filt PHI_leaf_filt
    ];
Vec2 = [ R_leaf_norm_filt TH_leaf_norm_filt PHI_leaf_norm_filt];

Incident_angles = angle_vec_sph_coord(Vec1,Vec2);
Sphcoord_leaf_filt= [TH_leaf_filt(:) PHI_leaf_filt(:) R_leaf_filt(:)];
Sphcoord_leafnorm_filt.TH_leaf_norm_filt = TH_leaf_norm_filt;
Sphcoord_leafnorm_filt.PHI_leaf_norm_filt = PHI_leaf_norm_filt;
Sphcoord_leafnorm_filt.R_leaf_norm_filt = R_leaf_norm_filt;

end
```

A.4 time_domain_impulse1.m

This function is to add up the individual transfer functions of leaves (realized by function get_echoes1.m) and then conduct inverse Fourier transform to get the time-domain signal.

```
% Inputs:
%         SONAR:
%         Sonargain: the sound amplitude each leaf receives from sonar
%
%         LEAF:
%         no_leaf, number of leaves
%         R_sonar_leaf, the distance between each leaf and sonar
%         leaf_dia, the radius of each leaf
%         Incident_angles, the vector of incident angles
%         echo_param, general info about echo, details please see
%         Sim_leaf_scattering.m
% Outputs:
%         impulse, the struct that contains the result and basic information
% Created by Chen Ming, Date: 06/01/2015
```

```
function impulse = time_domain_impulse1(Sonargain,R_sonar_leaf,leaf_dia,
    Incident_angles,echo_param)

a = leaf_dia(:);
theta0 = Incident_angles(:);
Fs = echo_param.Fs; % sampling frequency (kHz)
N = echo_param.Nbins; % no of bins b/w 60-80 kHz

% sonar inputs
pre_frq_a = 60; % in kHz
pre_frq_b = 80; % in kHz


delta_f = (Fs/N); % the interval in frequency domain is 0.01kHz
n = N/2; % In frequency domain, there are n + 1 bins.


no_bins = floor((pre_frq_b - pre_frq_a)/delta_f + 1); % Number of bins in the
    range that we are interested

w = hann(no_bins,'periodic'); % Apply a hanning window in frequency domain
    from 60kHz to 80kHz
w = repmat(w, 1, length(R_sonar_leaf(:)));


frq = pre_frq_a: delta_f :pre_frq_b;
[total_amp, total_phase] = get_echoes1(frq,a,theta0,no_bins,Sonargain(:),
    R_sonar_leaf(:));

ReX = total_amp.*cos(total_phase).*w;
ImX = total_amp.*sin(total_phase).*w;

% total ReX and ImX of all leaves
t_R = sum(ReX,2);
t_I = sum(ImX,2);


% add zeros in two ends of t_R and t_I
t_R = [zeros(1,floor(pre_frq_a/delta_f)), t_R', zeros(1,floor((Fs/2 -
    pre_frq_b)/delta_f))];
t_I = [zeros(1,floor(pre_frq_a/delta_f)), t_I', zeros(1,floor((Fs/2 -
    pre_frq_b)/delta_f))];

REX = t_R;
IMX = t_I;

for jj = n+2:N
    REX(jj) =  REX(N+2 -jj);
    IMX(jj) = -IMX(N+2 -jj);
end
```

```
XX = REX + 1i*IMX;
xx = ifft(XX);

% Here, there is an amplitude correction for hanning window function 2. For
    energy correction, the factor is sqrt(8/3);
impulse = 2.*xx; % Compensate for hanning window

end
```

A.5 get_echoes1.m

This program is to sum up the individual transfer functions of leaves.

```
% This program is to produce echoes from leaves
% Inputs:
%         frequency of the incident wave, frq, in kHz.
%
%         % LEAF INPUTS:
%         a, radius of the leaf
%         theta0, incident angle
%         Sonargain, the sound gain of each leaf from sonar
%         R_sonar_leaf, the distance between each leaf and sonar
%
%         % SONAR INPUTS:
%         frq, frequencies
%         no_bins, the number of bins in our interesting frequency range
%         [60, 80]kHz
% Outputs:
%         total_amp & total_phase, another interpretation of frequency domain
% Created by Chen Ming, Date: 06/01/2015

function [total_amp, total_phase] = get_echoes1(frq,a,theta0, no_bins,
    Sonargain,R_sonar_leaf)

%%% Calculate the total gain

% leaf beampatterns

[leaf_amp, leaf_phase] = leaf_beampattern( frq, a, theta0, no_bins);

%%% Calculate total amplitude gain
speed = 340;
lambda = speed./(frq*1E3);
k = 2*pi./lambda;
k = repmat(k',1,length(a));
dist_s_l = repmat(transpose(R_sonar_leaf(:)),no_bins,1);
sonar_gain = repmat(transpose(Sonargain(:)),no_bins,1);
```

```
total_amp = leaf_amp./(k.*dist_s_l).* sonar_gain.*0.2./dist_s_l;

%%% Calculate the total phase
total_phase = -2.*dist_s_l.*k - leaf_phase;

end
```

A.6 leaf_beampattern.m

This function is to calculate the transfer function of each leaf.

```
% This code is to describe the scattering of the leaves
% Inputs: frequency of incoming wave from the sonar, frq 60~80 (kHz)
%         radius of the leaf, a
%         incident angle, theta0, in radians
%         the number of bins between 60~80kHz, no_bins
% Outputs:
%          amplitude of the leaf beampattern, leaf_amp
%          phase of the leaf beampattern, leaf_phase
% Created by Chen Ming, Date: 06/01/2015

function [leaf_amp, leaf_phase] = leaf_beampattern(frq, a, theta0, no_bins)


%%% Amplitude of the leaf beampatterns
speed = 340;
lambda = speed./(frq*1E3);
k = 2*pi./lambda;
c = k'*a(:)';
Ac = 0.5003*c.^2 + 0.6867;

theta = repmat(transpose(theta0(:)),no_bins,1);

bc = 0.3999*c.^(-0.9065) +0.9979;
leaf_amp = Ac.*cos(bc.*theta);
leaf_amp(leaf_amp < 0) = 0;

%%% Phase of the leaf beampattern
pac = 0.9824*c.^0.3523 - 0.9459;
pbc = 2.6343;
leaf_phase = erf(pac.*(1.57-theta)) - pbc; % pac is a(c), pbc is b(c), which
   both describes the phase of the leaf beam pattern
end
```

A.7 predict_gauss_sigma.m

This function is to compute the spread of sonar's Gaussian beampattern

```
function [gauss_sigma ] = predict_gauss_sigma(input_type,input_value)
%PREDICT_GAUSS_SIGMA:Takes as input frequency of incdence & predicts the
%beamwidth for that frequency based on results from horseshoe bats or takes
   the beamwidth directly and then
%calculates the standard deviation for gauss beampattern
%Input:Beamwidth(-3dB) in degrees or Frequency(kHz): Only between 60-80 kHz
%Output:gauss_sigma:standard deviation for input frequency of incidence or
   beamwidth
%Created by:Anupam Kumar Gupta, Date: 01/03/2015

if (nargin < 2)
    error('Wrong number of inputs');
end
a = sqrt(2*(-log(0.7079)));
switch input_type
    case 'incident_freq'
        %%% Takes as input incident frequency in 60-80 kHz in kHz,
        %%% estimates beamwidth(-3dB) from horseshoe bat results and
        %%% calculates the standard deviation (spread) for gaussian
        %%% beampattern for estimated beamwidth

        f = input_value; % frequency b/w 60-80 kHz in kHz
        bmwdth = 0.011333*(f.^3) - 2.3219*(f.^2) + 156.15*f - 3402.7;
        gauss_sigma = 0.5*deg2rad(bmwdth)/a;

    case 'beamwidth'
        %%% Takes as input,beamwidth(-3dB) in degrees & predicts the
        %%% standard deviation (spread) for gaussian beampattern
        %%% for input beamwidth

        gauss_sigma = 0.5*deg2rad(input_value)/a;
end


end
```

A.8 gauss_beam_sonar.m

This program is to calculate the Gaussian beampattern

```
function [ Zgain ] = gauss_beam_sonar(amp,freqorbmwdth,freqorbmwdthVal,
   beamcenter,varargin)
%GAUSS_BEAM_SONAR: Gaussian approximation of actual bat beampatterns mainlobe
%Inputs: amp: Peak Amplitude of the beampattern
```

```
%        freqorbmwdth: 1) 'incident_freq' for entering frequency of incidence
%        b/w 60-80 kHz in kHz to estimate spread(sigma) of gauss beampattern
%        based on horseshoe data, 2) 'beamwidth' for directly entering
%        beamwidth in degrees and estimate spread(sigma) of gauss
%        beampattern for the same
%        freqorbmwdthVal: frequency (kHz) b/w 60-80 kHz for 'incident_freq' in
    freqorbmwdth
%        and beamwidth (degrees) for 'beamwidth' in freqorbmwdth.
%        center_x & center_y : coordinates of gaussian beam center
%        (default- 0,0), beamcenter
%
%        varagrin : add amplitude of gaussian white noise if needed
%Outputs: Zgain : gain matrix

% Make a 2D Gaussian Kernel in cartesian coordinates
A = amp;
x0 = beamcenter(1); y0 = beamcenter(2);

% Predict gaussian spread (standard deviation) based on horseshoe bat data
sigma_x = predict_gauss_sigma(freqorbmwdth,freqorbmwdthVal); % get sigma for
   beamwidth corresponding to frequency of incidence
sigma_y = predict_gauss_sigma(freqorbmwdth,freqorbmwdthVal); % get sigma for
   beamwidth corresponding to frequency of incidence

[X, Y] = meshgrid(linspace(-pi,pi,361),linspace(-pi/2,pi/2,181));

theta = 0;
a = ((cos(theta))^2)/(2*(sigma_x^2)) + ((sin(theta))^2)/(2*(sigma_y)^2);
b = (-sin(2*theta))/(4*(sigma_x)^2) + (sin(2*theta))/(4*(sigma_y)^2);
c = ((sin(theta))^2)/(2*(sigma_x)^2) + ((cos(theta))^2)/(2*(sigma_y)^2);
Z = A*exp( -((a*(X-x0).^2) + (2*b*(X-x0).*(Y-y0)) + (c*(Y-y0).^2)));
    if(~isempty(cell2mat(varargin)))
        %%% Add gaussian noise (white noise) to beampattern
        Znoise = (varargin{1})*randn(size(Z));
        Zgain = Z+Znoise;
    else
        Zgain = Z;
    end
end
```

A.9 angle_vec_sph_coord.m

Find angles between vectors in spherical coordinates.

```
function [ deltatheta ] = angle_vec_sph_coord(Vec1,Vec2)
% ANGLE_VEC_SPH_COORD: Find angle between vectors in spherical coordinate
% system by converting to cartesian coordinates and translating to origin.
% Created by: Anupam Kumar Gupta, Date: 02/25/2015
```

```
R_sonar = Vec1(:,1);
R_leaf = Vec1(:,4);
R_leaf_norm = Vec2(:,1);

TH_sonar = Vec1(:,2);
TH_leaf = Vec1(:,5);
TH_leaf_norm = Vec2(:,2);

PHI_sonar = Vec1(:,3);
PHI_leaf = Vec1(:,6);
PHI_leaf_norm = Vec2(:,3);

x1_strt = R_sonar .* cos(PHI_sonar) .* cos(TH_sonar);
x1_end =  R_leaf .* cos(PHI_leaf) .* cos(TH_leaf);

x2_end = R_leaf_norm .* cos(PHI_leaf_norm) .* cos(TH_leaf_norm);
x2_strt = zeros(size(R_leaf,1),1);


y1_strt = R_sonar .* cos(PHI_sonar) .* sin(TH_sonar);
y1_end = R_leaf .* cos(PHI_leaf) .* sin(TH_leaf);
y2_strt = zeros(size(R_leaf,1),1);
y2_end = R_leaf_norm .* cos(PHI_leaf_norm) .* sin(TH_leaf_norm);

z1_strt = R_sonar .* sin(PHI_sonar);
z1_end = R_leaf .* sin(PHI_leaf);
z2_strt = zeros(size(R_leaf,1),1);
z2_end = R_leaf_norm .* sin(PHI_leaf_norm);

A_strt = [x1_strt y1_strt z1_strt];
A_end = [x1_end y1_end z1_end];

B_strt = [x2_strt y2_strt z2_strt];
B_end = [x2_end y2_end z2_end];

A = A_end - A_strt;
B = B_end - B_strt;


ABdot = dot(A,B,2); % dot product between two vectors
ABcross = cross(A,B,2); % cross product between two vectors

ABcross_mag = sqrt(sum(ABcross.^2,2));

deltatheta =(abs(atan2(ABcross_mag,ABdot))); % angle between two vectors
indxanglegrt90 = find(deltatheta > pi/2);
deltatheta(indxanglegrt90) = pi - deltatheta(indxanglegrt90);

end
```

A.10 dist_points_sph_coord.m

Find distance between two points that are in spherical coordinates.

```
function [deltaR] = dist_points_sph_coord(r1,theta1,phi1,r2,theta2,phi2)
% DIST_POINTS_SPH_COORD: FInd distance between two points in spherical
%coordinates
% Created by: Anupam Kumar Gupta, Date: 02/24/2015

x1 = r1 .* cos(phi1) .* cos(theta1);
x2 = r2 .* cos(phi2) .* cos(theta2);
y1 = r1 .* cos(phi1) .* sin(theta1);
y2 = r2 .* cos(phi2) .* sin(theta2);
z1 = r1 .* sin(phi1);
z2 = r2 .* sin(phi2);

X = [x1 x2];
Y = [y1 y2];
Z = [z1 z2];

deltaR = sqrt((((diff(X,1,2)).^2) + ((diff(Y,1,2)).^2) + ((diff(Z,1,2)).^2)));
% deltaR = sqrt((x1 - x2)^2 + (y1 - y2)^2 + (z1 - z2)^2);

% deltaR = sqrt(r1^2 + r2^2 + - 2*r1*r2*((sin(phi1)*sin(phi2)*cos(theta1-
   theta2))+ (cos(phi1)*cos(phi2))));

end
```